Brain, Behavior, and Immunity 130 (2025) 106073

Contents lists available at ScienceDirect

Brain Behavior and Immunity

journal homepage: www.elsevier.com/locate/ybrbi

Full-length Article

Specific viral antibodies associate with anti-NMDAR encephalitis after herpes simplex encephalitis

Jakob Kreye [a,b,c,d,e,*], William R. Morgenlander [e], Manjusha Thakar [e], Poul M. Schulte-Frankenfeld [a,d], Sarah Schott [a,d], Isabel Bünger [a,b], Hans-Christian Kornau [c,f], Julia W. Angkeow [e], Sahana Jayaraman [e], Carolin Otto [b], Wiebke Hahn [g], Jan Lewerenz [h], Franziska S. Thaler [i], Mirjam Korporal-Kuhnke [j], Nico Melzer [k], Justina Dargvainiene [l], Christian G. Bien [m,n], Rose Kohlie [o], Erik Lattwein [o], Dietmar Schmitz [c,f], Peter A. Calabresi [p], Carlos A. Pardo [p], Harald Prüss [b,c], Klemens Ruprecht [b], H. Benjamin Larman [e,**]

[a] Charité – Universitätsmedizin Berlin, Corporate Member of Freie Universität Berlin and Humboldt-Universität zu Berlin, Department of Pediatric Neurology, Berlin, Germany
[b] Charité – Universitätsmedizin Berlin, Corporate Member of Freie Universität Berlin and Humboldt-Universität zu Berlin, Department of Neurology and Experimental Neurology, Berlin, Germany
[c] German Center for Neurodegenerative Diseases (DZNE) Berlin, Berlin, Germany
[d] Berlin Institute of Health at Charité – Universitätsmedizin Berlin, Germany
[e] Institute for Cell Engineering, Division of Immunology, Department of Pathology, Johns Hopkins University, Baltimore, MD, USA
[f] Charité – Universitätsmedizin Berlin, Corporate Member of Freie Universität Berlin and Humboldt-Universität zu Berlin, Neuroscience Research Center (NWFZ), Berlin, Germany
[g] Department of Neurology, Epilepsy Center, Philipps-University Marburg, Marburg, Germany
[h] Department of Neurology, Ulm University, Ulm, Germany
[i] Institute of Clinical Neuroimmunology, LMU University Hospital, LMU Munich, Biomedical Center (BMC), Faculty of Medicine, Germany
[j] Department of Neurology, University of Heidelberg, Heidelberg, Germany
[k] Department of Neurology, Medical Faculty and University Hospital, Heinrich Heine University of Düsseldorf, Düsseldorf, Germany
[l] Institute of Clinical Chemistry, University Hospital Schleswig-Holstein (UKSH), Christian-Albrechts-University (CAU), Kiel, Germany
[m] Department of Epileptology, Krankenhaus Mara, Bethel Epilepsy Center, Medical School OWL, Bielefeld University, Bielefeld, Germany
[n] Laboratory Krone, Bad Salzuflen, Germany
[o] Institute for Experimental Immunology, Affiliated with EUROIMMUN Medizinische Labordiagnostika AG, Lübeck, Germany
[p] Department of Neurology, Johns Hopkins University School of Medicine, Baltimore, MD, USA

ARTICLE INFO

Keywords:
MICAR
PhIP-Seq
Antibody reactome
Intrathecal synthesis
NMDAR
Encephalitis
HSV
HSE

ABSTRACT

Herpes simplex encephalitis (HSE) patients may develop secondary anti-N-methyl-D-aspartate receptor (NMDAR) encephalitis (NMDARE), associated with worsened long-term neurological outcome. Immunosuppressive treatment can limit NMDAR autoantibody-mediated pathology, but early predictive biomarkers for the risk of NMDARE are lacking. In a multicenter study, we performed unbiased antibody reactome profiling using Phage ImmunoPrecipitation Sequencing (PhIP-Seq). HSE patients with secondary NMDARE (n = 13) versus those without (n = 10) showed enhanced antibody responses against HSV-1, but not HSV-2, which comprised specific antibodies to five peptides of the HSV-1 UL42 and UL48 proteins. A score of these signature CSF antibodies identified HSE patients with secondary NMDARE with a sensitivity of 75%, a specificity of > 99%, a positive predictive value of 90%, a negative predictive value of > 97% and an odds ratio (OR) of 209 (CI: 28 – 1,582) across all individuals in this study, and with similar performance values in serum (>66%, >99%, >88%, >96%, OR 307 (15 – 6,089)). These signature antibodies represent a promising biomarker to identify HSE patients at risk for NMDARE development. In NMDARE patients without a history of HSE and in MS patients, no disease-associated HSV antibody reactivity patterns were detected. Furthermore, we introduced the Multiplexed Index Calculations of the Antibody Reactome (MICAR) metric to characterize proteomic targets of compartment-

* Corresponding author at: Department of Pediatric Neurology, Charité – Universitätsmedizin Berlin, corporate member of Freie Universität Berlin, Humboldt-Universität zu Berlin, and Berlin Institute of Health, Augustenburger Platz 1, 13353 Berlin, Germany.
** Corresponding author.
E-mail addresses: jakob.kreye@charite.de (J. Kreye), hlarman1@jhmi.edu (H. Benjamin Larman).

https://doi.org/10.1016/j.bbi.2025.106073
Received 2 April 2025; Received in revised form 15 July 2025; Accepted 9 August 2025
Available online 11 August 2025

specific antibody responses, an approach that is applicable in neuroimmunology and other compartmentalized disease states.

1. Introduction

Herpes simplex encephalitis (HSE) is the most common form of sporadic encephalitis, accounting for 15 to 40% of all encephalitis cases (George et al., 2014). The incidence is estimated at 2–12 patients per million inhabitants per year (George et al., 2014; Hjalmarsson et al., 2007; Jouan et al., 2015; Venkatesan et al., 2019). Even with the use of antiviral acyclovir treatment, HSE mortality rates range from 5 to 16% (Hjalmarsson et al., 2007; Jouan et al., 2015; Singh et al., 2016; Stahl et al., 2012), and HSE survivors frequently suffer from long-term neurological morbidity (Jouan et al., 2015; Sili et al., 2014). In addition to sequelae resulting from the infection itself, ~23% of HSE patients develop autoimmune encephalitis (AE) within 2 months of the onset of infection (Armangue et al., 2023; Armangue et al., 2018). HSE followed by a secondary AE is associated with worse neurological outcomes and higher long-term disabilities (Armangue et al., 2023).

In most AE post-HSE patients, N-methyl-D-aspartate receptor (NMDAR) autoantibodies are found (Armangue et al., 2023; Armangue et al., 2018; Pruss et al., 2012), which cause reversible NMDAR dysfunction (Ceanga et al., 2023; Hughes et al., 2010; Hunter et al., 2024; Kreye et al., 2016; Planaguma et al., 2015; Wright et al., 2021) and mark the most frequent form of AE, known as anti-NMDAR encephalitis (NMDARE) (Dalmau and Graus, 2018; Dalmau et al., 2007). Other NMDARE cases have been reported in association with ovarian teratomas, although the majority are idiopathic (Dalmau et al., 2007; Nosadini et al., 2021). Despite the severity of clinical presentation that commonly involves psychosis, seizures and autonomic dysfunction, NMDARE patients generally achieve remarkable improvement with adequate immunosuppressive therapies, often with complete remission (Titulaer et al., 2013). In contrast, delayed treatment initiation correlates with poor outcomes (Nosadini et al., 2021). This suggests that for HSE patients progressing to NMDARE, the outcome may be improved by earlier immunosuppressive treatments. However, timely differentiation of HSE patients developing secondary NMDARE (H+N+) from those who do not (H_{only}) is challenging for several reasons. First, clinical signs of secondary autoimmunity often resemble residual infection-related symptoms or those from viral reactivation, particularly in older children and adults, who may present with isolated behavioral abnormalities without movement disorders (Armangue et al., 2015; Bradshaw and Venkatesan, 2016; Nosadini et al., 2017). Second, transient NMDAR autoantibodies have been reported in individuals without the clinical picture of AE (Armangue et al., 2023; Dahm et al., 2014; Hansen et al., 2013; Pruss et al., 2012). Third, the underlying etiology of NMDARE post-HSE is insufficiently understood, and no predictive biomarkers are available (Dalmau et al., 2019). A recent study found prolonged interferon type I responses in H+N+ patients compared to H_{only} (Armangue et al., 2023). However, interferon-related gene signatures were increased in only one of four time points tested and were non-specific to post-HSE AE, limiting their clinical utility.

We hypothesized a heightened and/or differential herpes simplex virus (HSV) antibody response in H+N+ patients and aimed to characterize specific features of the antibody response that may serve as clinically useful biomarkers for risk of post-infectious NMDARE. Such antibody biomarkers might include differential patterns of binding to the viral proteome and/or differential levels of intrathecal antibody synthesis (ITAS or ITS). ITS refers to antibody production in the central nervous system (CNS) (Reiber and Felgenhauer, 1987), with antigen-specific ITS being a characteristic feature of viral and autoimmune encephalitis (Hummert et al., 2023; Pruss, 2021; Shamier et al., 2021). However, currently available diagnostics can only quantify ITS for one or a small number of antibody specificities at a time (single-plex or oligo-plex) (Leypoldt et al., 2015; Reiber and Felgenhauer, 1987; Reiber and Lange, 1991). In contrast, we here use Phage ImmunoPrecipitation Sequencing (PhIP-Seq) technology (Larman et al., 2013; Larman et al., 2011; Xu et al., 2015) in combination with a novel metric, Multiplexed Index Calculations of the Antibody Reactome (MICAR), to quantify ITS for hundreds or thousands of antibody reactivities simultaneously. We present an analysis of antibody reactivities in H+N+ and H_{only} patients, along with NMDARE patients without a history of HSE (N_{only}) and multiple sclerosis (MS) patients as controls.

2. Materials and methods

2.2. Patient cohorts and biospecimens

We identified NMDARE and HSE patients with available biospecimens retrospectively through a proposal to the GErman NEtwork for Research on AuToimmune Encephalitis (GENERATE network, generate-net.de) and to Johns Hopkins School of Medicine in 2023, and recruited from a total of 17 study centers. For HSE, patient inclusion was based on a documented history of CNS infection with HSV and corresponding clinical and imaging data. For NMDARE, patient inclusion was based on published criteria for definite NMDARE (Graus et al., 2016), with diagnosis determined by clinical features and not solely on the presence of NMDAR antibodies. In fact, one H_{only} patient had transient serum NMDAR antibodies at low titers in the initial phase of HSE without clinical picture of NMDARE, a phenomenon also described in a recent prospective cohort (Armangue et al., 2023). With regard to the partial overlap of HSE and NMDARE, the respective patients were grouped into three cohorts as follows: i) individuals with HSE and secondary NMDARE (H+N+), ii) individuals with HSE without evidence of NMDARE (H_{only}), and iii) individuals with NMDARE without a history of HSE (N_{only}). In the H+N+ cohort, samples can be from time points before, at or after NMDARE was diagnosed. Follow-ups were similar in HSE cohorts according to study center standards and at least > 3 months after HSE onset to enable proper differentiation between H+N+ and H_{only} individuals. MS was selected as a neuroimmunological control cohort. Patients were recruited at Charité – Universitätsmedizin Berlin with diagnosis based on McDonald criteria of 2017 (Thompson et al., 2018). The patients ranged in age from 3 months to 94 years (median: 34 years), including 7 children and 126 adults. The final size of the study cohort was determined by the availability of biospecimens.

2.3. Biospecimen collection

All samples were collected during routine diagnostic work-up at respective study centers between 2005 and 2023. Samples were promptly frozen and stored at −80 °C until further use. To avoid potential interference, all patients who had received intravenous immunoglobulin treatment within six months prior to sampling were excluded. No other exclusion criteria were applied. For study investigations, a total of 309 samples from 133 individuals were included, comprising n = 41 (21 CSF, 20 serum, of which 20 are CSF/serum pairs) from 13 H+N+ individuals, n = 18 (11 CSF, 7 serum, of which 6 are CSF/serum pairs) from 10 H_{only} individuals, n = 170 (86 CSF, 84 serum, of which 82 are CSF/serum pairs) from 70 N_{only} individuals and n = 80 (40 CSF, 40 serum, of which 40 are CSF/serum pairs) from 40 patients with MS. H+N+ samples are from time points before (5 CSF, 4 serum, of which 4 are CSF/serum pairs), at (3 CSF, 3 serum, of which 3 are CSF/serum pairs), or after (13 CSF, 13 serum, of which 13 are CSF/serum pairs) NMDARE manifestation. All CSF and serum sample pairs were collected on the same day.

2.4. Immunodiagnostic parameters and intrathecal synthesis calculation

Measurement of basic laboratory parameters, including CSF white blood cell counts, CSF/serum albumin and immunoglobulin G (IgG) antibody levels, as well as OCB evaluation, were performed locally at study centers as part of routine clinical diagnostics. Type 2 and 3 OCBs were considered CSF-specific OCBs, following consensus recommendations (Andersson et al., 1994). From the CSF/serum albumin ratio (Q_{Alb}), the age-adjusted CSF/serum albumin ratio (age-adjusted Q_{Alb}) was determined by dividing Q_{Alb} by the age-dependent upper limit ($Q_{lim(Alb)}$, 4 + age/15, with age in years). From the CSF/serum IgG ratio (Q_{IgG}), the clinical ITS of total IgG was considered positive if $Q_{IgG} > Q_{lim(IgG)}$, with $Q_{lim(IgG)}$ determined using the hyperbolic function $Q_{lim(IgG)} = 0.93*\sqrt{(Q_{Alb}^2 + 6*10^{-6})} - 1.7*10^{-3}$. If positive, the clinical ITS of total IgG was determined as ITS [in %] = $(Q_{IgG} - Q_{lim(IgG)})/Q_{lim(IgG)})$. If the clinical ITS of total IgG was calculated to be negative ($Q_{IgG} \leq Q_{lim(IgG)}$), it was set to 0%, all following previously established definitions (Reiber, 1998).

2.5. NMDAR Cell-based assay (CBA)

NMDAR antibody titers were obtained from routine diagnostic CBAs and indicated as routine tests in Fig. S1. Those tests were performed locally at study centers using different CBAs, including live or fixed cells, and different dilution steps. For standardized re-tests, all samples were subjected to a secondary evaluation at a reference laboratory, using human embryonic kidney 293 (HEK293T) cells transfected with NMDAR1, following established protocols and according to the manufacturer's instructions for use (Anti-Glutamate receptor (type NMDA) IIFT, FA 112d-1010–51, EUROIMMMUN Medizinische Labordiagnostika AG) (Dalmau et al., 2008; Dalmau et al., 2007). Lowest dilutions were 1:1 for CSF and 1:10 for serum samples.

2.6. Phage immunoprecipitation sequencing (PhIP-Seq) experiments

PhIP-Seq experiments were performed following established protocols (Mohan et al., 2018). For IgG antibody reactome analyses against tiled proteomes of human viruses, including HSVs, the VirScan phage library (110,215 56-mer peptides) (Xu et al., 2015), was used. Additionally, to enable the computation of intrathecal synthesis of specific reactivities from a broader reactome data set (MICAR paragraph below), further phage libraries were included, which display proteomes of humans (HuScan, 274,207 90-mer peptides) (Larman et al., 2011; Xu et al., 2016), protein allergens (AllerScan, 19,331 56-mer peptides) (Monaco et al., 2021), environmental toxins and virulence factors (ToxScan, 95,601 56-mer peptides) (Angkeow et al., 2022), and bacteriophages (PhageScan, 100,275 56-mer peptides) (Liebhoff et al., 2024). In brief, for incubation of patients' IgG antibodies with PhIP-Seq libraries, CSF and serum samples were randomly assigned to four 96-well plates with equal distribution of cohorts across plates. Paired samples were processed on the same plate. To adjust for difference in IgG levels in serum versus CSF, we diluted samples to 2 μg of IgG if possible, with rounded volumes capped at a maximum of 40 μL. For CSF, 52 samples contained 2 μg ± 20% (mean 2.00 μg and median 1.99 μg), 81 samples contained < 1.6 μg (mean 0.82 μg and median 0.81 μg) and 25 samples had unknown IgG concentrations. For serum, 128 samples contained 2 μg ± 20% (mean 1.99 μg and median 1.98 μg) and 23 samples had unknown IgG concentrations. The antibody-phage mixture was kept shaking overnight at 4 °C, then incubated with protein A and protein G coated magnetic beads (Dynabeads, Invitrogen) to immunocapture IgG-bound phage. The peptide coding sequences of the captured phage were amplified for Illumina sequencing using two lanes of a NovaSeq SP 100 flow cell with an estimated coverage of approximately 3.5 reads per peptide.

2.7. PhIP-Seq analytics

Fastq files were aligned to quantify peptide-corresponding read counts for all peptides, but excluding those corresponding to the Human Immunodeficiency Virus (HIV), as HIV-antibody testing requires a separate written consent under the German Infection Protection Act, which was not obtained from all study participants. For each peptide, antibody reactivity was measured as fold-change binding versus control conditions with no sample input ("mock IP"), and referred to relative binding throughout the manuscript. Following established protocols (Larman et al., 2011; Mohan et al., 2018), P-values of differential abundance were calculated separately for each peptide using the EdgeR software and antibody reactivities to peptides were considered significant and referred to as a "hit" if the read count in the sample was at least 15, the relative binding was at least 5-fold over bead-controls, and the P-value was below 0.001. Samples were excluded from further analysis if total peptide hits were below 250 (two serum and one CSF sample) or maximum relative binding was below 40 (one additional serum). Correctness of CSF/serum sample pairing was evaluated by correlating public peptide reactivities of VirScan and ToxScan libraries (Angkeow et al., 2022) and by excluding discordant pairs from further analysis if the Pearson's correlation coefficient was below 0.6 (one CSF/serum pair). To evaluate antibody responses at the viral species level (e.g. Fig. 5A), virus aggregate reactivity scores (VARscores) were computed by comparing average fold-change binding of the peptides associated with each virus versus distributions of randomly selected peptides (Morgenlander, 2022), and by using a threshold of positivity at 0.72 to define seropositivity (Morgenlander et al., 2024). The breadth of an antibody response to a virus (e.g. Fig. 4B) was measured as the count of virus-specific peptide hits (including such with partial overlap). For quantification of the strength of an antibody reactivity to entire viruses (e.g. Fig. 4D), the virus-specific relative binding was measured as the mean relative binding of five peptides representing the respective virus, using the highest relative binding values of five peptides from five different viral proteins.

2.8. Multiplexed Index Calculations of the Antibody Reactome (MICAR)

In this study, we introduce and establish MICAR, a novel algorithm for quantifying intrathecal synthesis based on multiplexed antibody reactivity profiles obtained via PhIP-Seq. MICAR scoring uses paired relative binding values (fold-change binding versus mock IP controls with no sample input), analogous to routine-diagnostic antibody indices (Reiber and Lange, 1991). MICAR scores were computed for relative binding values from PhIP-Seq data for paired CSF and serum samples (MICAR indices, representing a quantification for ITS). We implemented MICAR readouts as equivalents for clinical ITS of total IgG (referred to as "MICAR ITS of total IgG"), virus-specific ITS (referred to as "MICAR virus antibody indices"), and peptide-specific ITS (referred to as "MICAR peptide antibody indices"). MICAR incorporates normalization that accounts for differences in the IgG input. For this purpose, MICAR peptide antibody indices are ratios of relative binding for each peptide adjusted by the ratio of median relative binding for all peptide hits from the CSF (1,145 ± 499 hits from five phage libraries, mean ± standard deviation). Considering the ratio of median relative binding for all peptide hits is analogous to the correction by the total IgG amount in conventional ELISA-based antibody index calculations (Shamier et al., 2021). In brief, MICAR peptide antibody indices for paired CSF and serum relative binding values (fold-change versus mock IP controls with no sample input) are calculated as:

$$\text{MICAR peptide antibody index} = \frac{\frac{\text{Relative binding}_{CSF}[\text{peptide}]}{\text{Relative binding}_{serum}[\text{peptide}]}}{\frac{\text{Median relative binding}_{CSF}[\text{all peptide hits}_{CSF}]}{\text{Median relative binding}_{serum}[\text{all peptide hits}_{CSF}]}}$$

For MICAR peptide antibody indices, MICAR indices are considered positive (MICAR+) if i) the peptide reactivity is considered a hit in the

CSF, ii) the mean of the paired relative binding values is > 3, and iii) the ratio of the paired relative binding value is also > 3. Peptide antibody reactivities that are a CSF hit but are not MICAR+ are annotated as MICAR- peptides. For MICAR virus antibody indices, the mean of MICAR peptide antibody indices was computed for all viruses with five or more peptide hits in the CSF. For MICAR ITS of total IgG, the count of MICAR+ peptide was divided by the total count of peptide hits in the CSF (including MICAR+ and MICAR- peptides). Similar to the clinical ITS of total IgG parameter, MICAR ITS of total IgG indicates to what degree CSF antibodies are intrathecal antibodies, i.e. derive from production within the CNS. For inversed MICAR scoring (Fig. S3D-F), the same calculations were applied except with values from CSF and serum interchanged.

In addition, when analyzing the relative binding values for both compartments separately (and not their ratio), a normalization factor, defined as the square root of the ratio of median relative binding for the CSF and the serum reactomes, was applied. For normalized relative binding values in the CSF, relative binding values are divided by the normalization factor, as:

$$\text{Normalized relative binding}_{\text{CSF}} = \frac{\text{Relative binding}_{\text{CSF}}}{\sqrt[2]{\frac{\text{Median relative binding}_{\text{CSF}}[\text{all peptide hits}_{\text{CSF}}]}{\text{Median relative binding}_{\text{serum}}[\text{all peptide hits}_{\text{CSF}}]}}}$$

For normalized relative binding values in the serum, relative binding values are multiplied by the normalization factor, as:

$$\text{Normalized relative binding}_{\text{serum}} = \text{Relative binding}_{\text{serum}} \times \sqrt[2]{\frac{\text{Median relative binding}_{\text{CSF}}[\text{all peptide hits}_{\text{CSF}}]}{\text{Median relative binding}_{\text{serum}}[\text{all peptide hits}_{\text{CSF}}]}}$$

2.9. UL42 and UL48 signature antibodies

The UL42-UL48-antibody score condenses the cumulative antibody binding against the five herpes simplex virus type 1 (HSV-1) "signature peptides" into a single metric (e.g. Fig. 4I-K). The score was defined as the sum of relative binding values from PhIP-Seq data (fold-change versus mock IP controls with no sample input) of the five signature peptides, with a minimum value of 5 (if none of the peptides are considered a hit, since each peptide will have a fold-change of 1). In a receiver-operating characteristic curve (ROC) analysis using the pROC package in R, a sum-based scoring metric of the individual binding values revealed superior discriminative performance to differentiate H+N+ individuals from other disease groups (area under the curve, AUC = 0.869 for CSF samples) versus a median-based scoring approach (AUC = 0.708 for CSF samples), and was therefore selected for all subsequent analyses. The optimal cut-off was determined on scores from all individuals of the study cohort using Youden Index computation and defined at 38.8 for CSF samples (sensitivity 75%, specificity > 99%) and at 15.3 for serum samples (sensitivity > 66%, specificity > 99%).

For validation, a signature antibody ELISA was performed using with the five signature peptides synthesized by Biomatik (Ontario, Canada) and following established procedures (Bunger et al., 2023). In brief, the peptides were diluted in PBS and pooled isomolar to a total peptide concentration of 2 μg/ml, then incubated overnight at 4 °C in 96-well high-binding plates. The plates were then blocked for 1 h with PBS containing 1% BSA and 0.05% Tween, before incubating sera diluted 1:200 in blocking solution for another hour. After washing, an ALP-coupled anti-human IgG antibody (Mabtech, #3850-9A-1000) was added for 1 h, before development using pNPP substrate solution and recording of 405 nm absorbance values after 30 min. The optimal cut-off was determined on measurements from all H+N+ and H_{only} individuals using Youden Index computation and defined at an optical density of 0.1095 for serum samples (after subtracting the sample-specific optical density measured without preincubation with the signature peptides).

2.10. Protein sequence comparison

For HSV-1 and NMDAR sequence comparison, UniProt full-length protein sequences for HSV's UL42 (UniProt accession P10226) and UL48 (P06492) were compared with the NMDAR subunit 1 (Q05586) using the MEME sequence analysis tool for ungapped motifs (meme-suite.org) (Bailey and Elkan, 1994; Bailey et al., 2015). MEME provides so called E-values for each motif, which are based on its log likelihood ratio, width, sites, the background amino acid frequencies, and the size of the training set. We considered motifs as statistically significant with an E-value < 0.05, following the authors' recommendations (Bailey et al., 2015).

2.11. Statistical analysis

All analyses were performed using RStudio 2023.06.1 (Posit Software, PBC) and GraphPad Prism 9.5.1 (GraphPad Software). For statistical tests, unless indicated otherwise, only one sample per individual was used, selected from the earliest sampling time point if multiple were available. For each individual test, missing data points were not considered for the respective comparison. For the investigations of differential patterns in antibody responses between the H+N+ and H_{only} cohorts (Fig. 4, Fig. S5, Fig. S6, Table S2, Table S3), the first time points > 14 days after HSE onset were used (to account for time required to develop an antibody response after infection), and in the H+N+ cohort, the first sample after NMDARE manifestation was used, if available. Unpaired quantitative data were analyzed using unpaired t-tests if data were parametric or Mann-Whitney tests if non-parametric. Paired quantitative data were analyzed using paired t-tests if data were parametric or Wilcoxon tests if non-parametric. For comparison of quantitative data from more than two groups, one-way ANOVA tests with post-hoc Tukey's multiple comparisons were performed if data were parametric, and Kruskal-Wallis tests with post-hoc multiple comparisons using Dunn's test were performed if data were non-parametric. The significance level for the indicated statistical plots is indicated in the plots as follows: * $P < 0.05$, ** $P < 0.01$, *** $P < 0.001$, **** $P < 0.0001$, or is not significant if not shown. Linear correlations of two variables were determined using Pearson correlation models (GraphPad Prism). All P-values are two-tailed and were considered statistically significant if < 0.05. For UL42-UL48-antibody score performance evaluation, sensitivity was calculated as true positives/(true positives + false negatives), specificity as true negatives/(true negatives + false positives), the PPV as true positives/(true positives + false positives) and NPV as true negatives/(true negatives + false negatives). Odds ratios (OR) and corresponding 95% confidence intervals (CI) were calculated from 2x2 contingency tables using the Haldane–Anscombe correction.

3. Results

3.1. A subset of HSV antibodies is detected only in CSF in HSE

To investigate if HSE patients who go on to develop NMDARE produce heightened and/or differential HSV antibody responses, we collected 309 CSF and serum samples (including 148 pairs) from 133

Table 1
Demographics and routine diagnostic CSF results from study cohorts.

	HSE and NMDARE (H+N+)	HSE w/o NMDARE (H_{only})	NMDARE w/o HSE (N_{only})	Multiple Sclerosis (MS)
Patients, *n*	13	10	70	40
Samples (CSF, serum, thereof CSF/serum pairs), count	21, 20, 20	11, 7, 6	86, 84, 82	40, 40, 40
Age, in years, median (IQR)	64 (38–75)	36 (25.8–60)	29 (21–36)	33.5 (28.3–38.8)
Female, count (%)	8 (61.5%)	5 (50.0%)	53 (75.7%)	27 (67.5%)
Time point of sampling[a], in months[b], median (IQR)	2 (0.5–6.5)	6.5 (0.0–44.3)	8 (0.6–24)	6 (1–23)
WBC[a], in cells/µl, median (IQR)	9 (2.3–127.5)	12 (4.5–143)	3 (1–10.5)	10 (5.3–17.8)
Age-adjusted Q_{Alb}[a], as ratio, median (IQR)	0.81 (0.62–2.3)	0.65 (0.43–1.8)	0.70 (0.50–1.0)	0.70 (0.50–0.90)
Age-adjusted Q_{Alb} > 1[a], count (%)	4 (33.3%)	3 (42.9%)	17 (25.4%)	6 (15.0%)
Intrathecal IgG synthesis[a], in %, median (IQR)	24.5 (0–43)	0 (0–19.5)	0 (0–7)	25 (8.5–46.5)
Intrathecal IgG synthesis > 0%[a], count (%)	7 (58.3%)	2 (25.0%)	17 (25.8%)	31 (77.5%)
CSF-specific OCBs[a], count (%)	8 (61.5%)	5 (62.5%)	30 (44.8%)	40 (100%)
Serum NMDAR-IgG titer[a], median (IQR)	7.5 (*neg*[c,d]-77.5)	*neg*[c] (*neg*[c]-*neg*[c])	50 (10–320)	*neg*[c] (*neg*[c]-*neg*[c])
CSF NMDAR-IgG titer[a], median (IQR)	1 (*neg*[c,d]-10)	*neg*[c] (*neg*[c]-*neg*[c])	10 (1–64)	*neg*[c] (*neg*[c]-*neg*[c])

IQR = interquartile range, Q_{Alb} = CSF/serum albumin ratio, WBC = white blood count.

[a] Data is from earliest available sample for each individual.

[b] Time is measured in months after onset of first disease-associated symptoms. For H+N+ patients, this refers to the onset of HSE symptoms.

[c] *neg* indicates that CBA for NMDAR-IgG was negative in the initial dilution tested (1:10 for serum, 1:1 i.e. undiluted for CSF samples).

[d] Some H+N+ patients tested negative for NMDAR-IgG in earliest available sample (shown here), all tested positive at later time points of sampling.

patients with HSE (59 samples, 23 patients), NMDARE (170 samples, 70 patients), and MS (80 samples, 40 patients). The HSE patients were divided into individuals with (H+N+, 41 samples, 13 patients) or without (H_{only},18 samples, 10 patients) secondary NMDARE. Further NMDARE patients are those without a history of HSE (N_{only}). MS patients were included as controls. In all four cohorts, samples were obtained at similar intervals after symptom onset. Age, sex distribution, and routine laboratory CSF test results corresponded with disease-typical features (Table 1). Preexisting autoimmune comorbidities, disease course and antiviral treatments were not significantly different between the H+N+ and H_{only} groups (Table S1).

For quality assurance, we first quantified NMDAR antibodies in all samples. We found strong correlation between titers from previous (routine diagnostics) and current NMDAR-IgG tests, indicating that sample pairs are suitable for comparative antibody analysis even after long-term storage (Table 1, Fig. S1). Next, we performed PhIP-Seq measurements using five phage libraries to comprehensively profile IgG antibody binding reactivities against the HSV proteome and nearly 600,000 peptides from proteomes of human viruses (VirScan) (Xu et al., 2015), humans (HuScan) (Larman et al., 2011; Xu et al., 2016), protein allergens (AllerScan) (Monaco et al., 2021), environmental protein toxins and virulence factors (ToxScan) (Angkeow et al., 2022), and bacteriophages (PhageScan) (Liebhoff et al., 2024). IgG antibody reactomes were captured from 2 µg of IgG whenever possible and at an average sequencing depth of ~ 2.1 million reads per sample. Across the four disease cohorts, the antibody reactomes were similar in numbers of total peptide targets (hits), median level of reactivity, and maximum level of reactivity (Fig. S2A-H), suggesting comparable humoral immune competence across groups. For CSF/serum pairs, on average, approximately half of all antibody hits were shared between CSF and serum antibody reactomes. Among the remainder, there were more serum-exclusive than CSF-exclusive hits (Fig. 1A, Fig. S2I-J). The total number of CSF-exclusive hits and those that correspond to HSV-1 and HSV-2 were increased in the H+N+ but not in the H_{only} cohort when compared to patients without a history of HSE (Fig. 1B-C). However, we observed that CSF-exclusive hits (as well as serum-exclusive hits) include predominantly weak reactivities in contrast to shared hits. We considered that intrathecal antibodies include those that are CSF-exclusive (likely weakly binding in CSF and undetectable in serum) and those that are CSF-enriched (strongly binding in CSF and co-detected in serum). Therefore, for complete characterization of intrathecal antibodies that include strongly binding, CSF-enriched antibodies, a quantitative comparison of antibody-compartment responses is required.

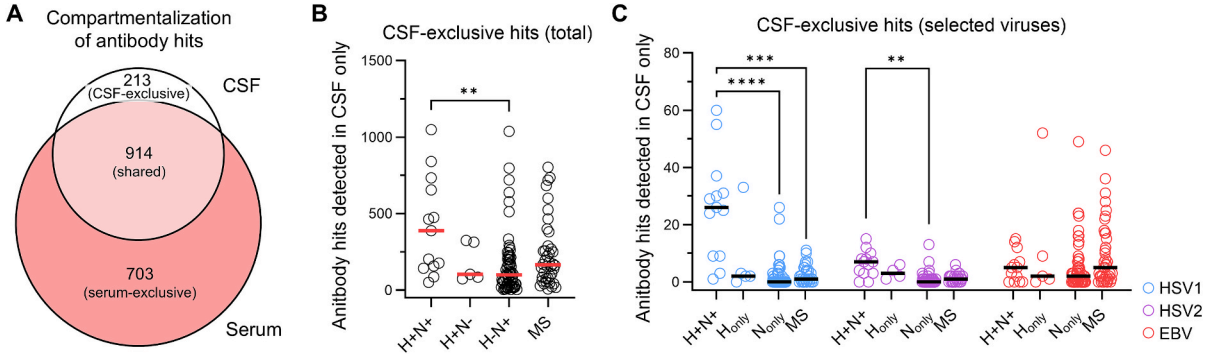

Fig. 1. CSF-exclusive HSV antibody reactivities. (A) A Venn diagram is shown to illustrate the overlap of the total antibody hits from paired CSF/serum samples. Numbers and relative areas represent mean values from data of n = 123 sample pairs from all four disease cohorts. (B) Scattered dot plots display counts of CSF-exclusive antibody hits (for peptides from all PhIP-Seq libraries) (n = 123 paired CSF/serum samples). Hits are considered CSF-exclusive if antibody binding was detected by CSF antibodies but not by serum antibodies. Red bars indicate median. For comparison, a Kruskal-Wallis test with post-hoc multiple comparisons using Dunn's test was performed. (C) For selected viruses, scattered dot plots display counts of CSF-exclusive antibody hits (n = 123 paired CSF/serum samples, shown only if total virus-specific hits are ≥ 10). Black bars indicate median. For comparison, a Kruskal-Wallis test with post-hoc multiple comparisons using Dunn's test was performed. (For interpretation of the references to color in this figure legend, the reader is referred to the web version of this article.)

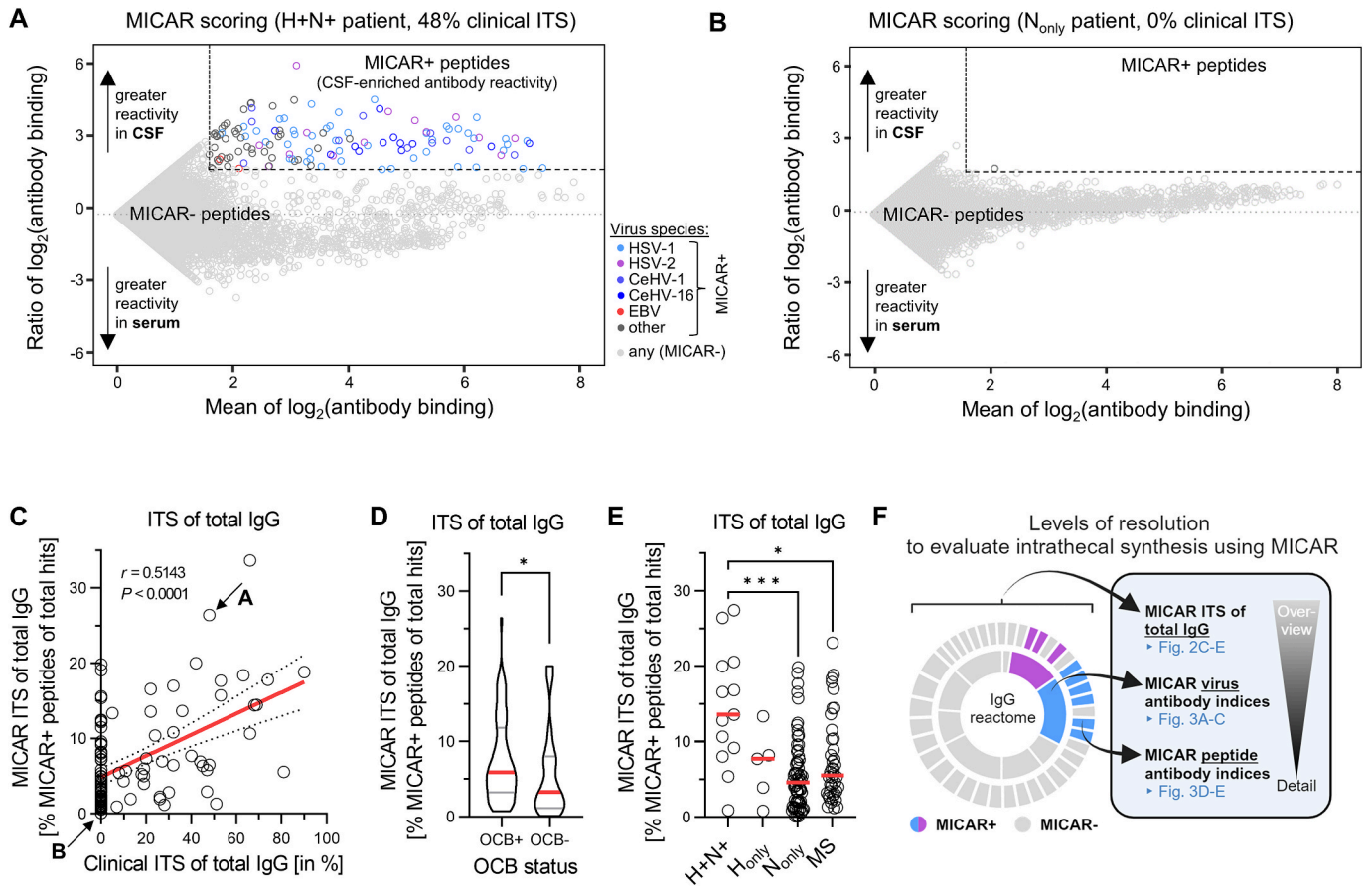

Fig. 2. Multiplexed Index Calculations of the Antibody Reactome (MICAR) correlates with clinical ITS. (A and B) Examples of MICAR scoring for IgG antibody binding to viral peptides are shown for (A) an H+N+ patient with pronounced ITS and for (B) a N_{only} patient with negative clinical ITS of total IgG. MICAR indices for CSF/serum pairs are considered positive (indicating intrathecal antibodies, MICAR+, dashed box), if the mean and the CSF/serum-ratio of the normalized relative binding values are > 3, or > 1.58 in log_2-scale (Methods). All viral peptides from the VirScan PhIP-Seq library (n = 110,215) are displayed, MICAR+ peptides representing selected viruses are highlighted by color. (C) A Pearson correlation model is shown that measures linear correlation between the MICAR ITS of total IgG and the clinical ITS of total IgG (n = 111 CSF/serum sample pairs with available clinical data). Dotted lines indicate 95 % CI. MICAR ITS of total IgG was determined as the count of MICAR+ peptides relative to total CSF peptide hits using peptides from all PhIP-Seq libraries (n = 599,629). Arrows indicate the individuals shown in A and B. (D) Truncated violin plots display MICAR ITS of total IgG from CSF/serum pairs, separately for pairs with (n = 64) and pairs without (n = 35) CSF-specific OCBs. Red lines indicate median, grey lines indicate interquartile range. For comparison, a Mann-Whitney test was performed. (E) Scattered dot plots display MICAR ITS of total IgG (n = 123 paired CSF/serum samples). Red bars indicate median. For comparison, a Kruskal-Wallis test with post-hoc multiple comparisons using Dunn's test was performed. (F) A cartoon illustrating depths of resolution of MICAR scoring to identify ITS of total IgG, and at level of virus species and proteomic peptide libraries. (For interpretation of the references to color in this figure legend, the reader is referred to the web version of this article.)

3.2. Multiplexed index calculations reveal intrathecal HSV antibody reactomes

Previous PhIP-Seq investigations had not quantitatively analyzed pairwise compartment comparisons (Johnson et al., 2019). We therefore developed a novel metric called Multiplexed Index Calculations of the Antibody Reactome (MICAR). MICAR scoring allows differentiation of whether peptides are targeted by intrathecal antibodies (MICAR+) or by antibodies equally present in CSF and serum (MICAR-) (Fig. 2A-B). The MICAR algorithm (Methods) is robust to differences in the IgG input and uses optimized thresholds to define MICAR-positivity (Fig. S3A-B).

Within this study's cohorts, we observed striking variability in the quantity of MICAR+ peptide hits, ranging from 1 to 551 peptides. As expected, the fraction of MICAR+ peptide hits, referred to as "the MICAR ITS of total IgG", correlated well with the clinical measures of ITS, i.e. the fraction of the IgG produced in the CSF among the total IgG (called "clinical ITS of total IgG") and the presence of CSF-specific oligoclonal bands (OCBs, another clinically used measure for the detection of ITS) (Fig. 2C-D). When using MICAR scoring to detect serum-enriched instead of CSF-enriched antibody responses ("inversed MICAR"), as expected we found the fraction of MICAR+ peptide hits to be low and not correlated with clinical ITS of total IgG or OCB status (Fig. S3C-F). These results are consistent with the fact that the majority of IgG in the CSF is physiologically derived from peripheral immune responses and diffuses into the CNS. If present, additional oligoclonal IgG in the CSF derives from ITS. Across the four cohorts, MICAR ITS of total IgG was highest in the H+N+ cohort (Fig. 2E), similar to the clinical ITS of total IgG measurements (Table 1). However, in contrast to the clinical ITS test, the MICAR approach also reveals the proteomic targets of intrathecal antibodies at virus-specific and at peptide-specific resolution (Fig. 2F).

In the H+N+ cohort, the MICAR+ reactome revealed a predominance of viral peptides (Fig. S3G). Therefore, we next aimed to implement MICAR comparison at the level of virus species, equivalent to clinically used diagnostics (Reiber and Lange, 1991; Shamier et al., 2021; Warnke et al., 2014), but at a breadth of all human viruses. To compute virus-specific ITS (MICAR virus antibody indices), we aggregated MICAR peptide antibody indices of the corresponding peptides (Methods) and found greater MICAR+ virus indices in patients with positive clinical ITS of total IgG and those with CSF-specific OCBs (Fig. S4A-B), supporting the validity of the approach. Interestingly, even in H+N+ and H_{only} patients with negative clinical ITS of total IgG and those without OCBs, we frequently detected positive MICAR virus

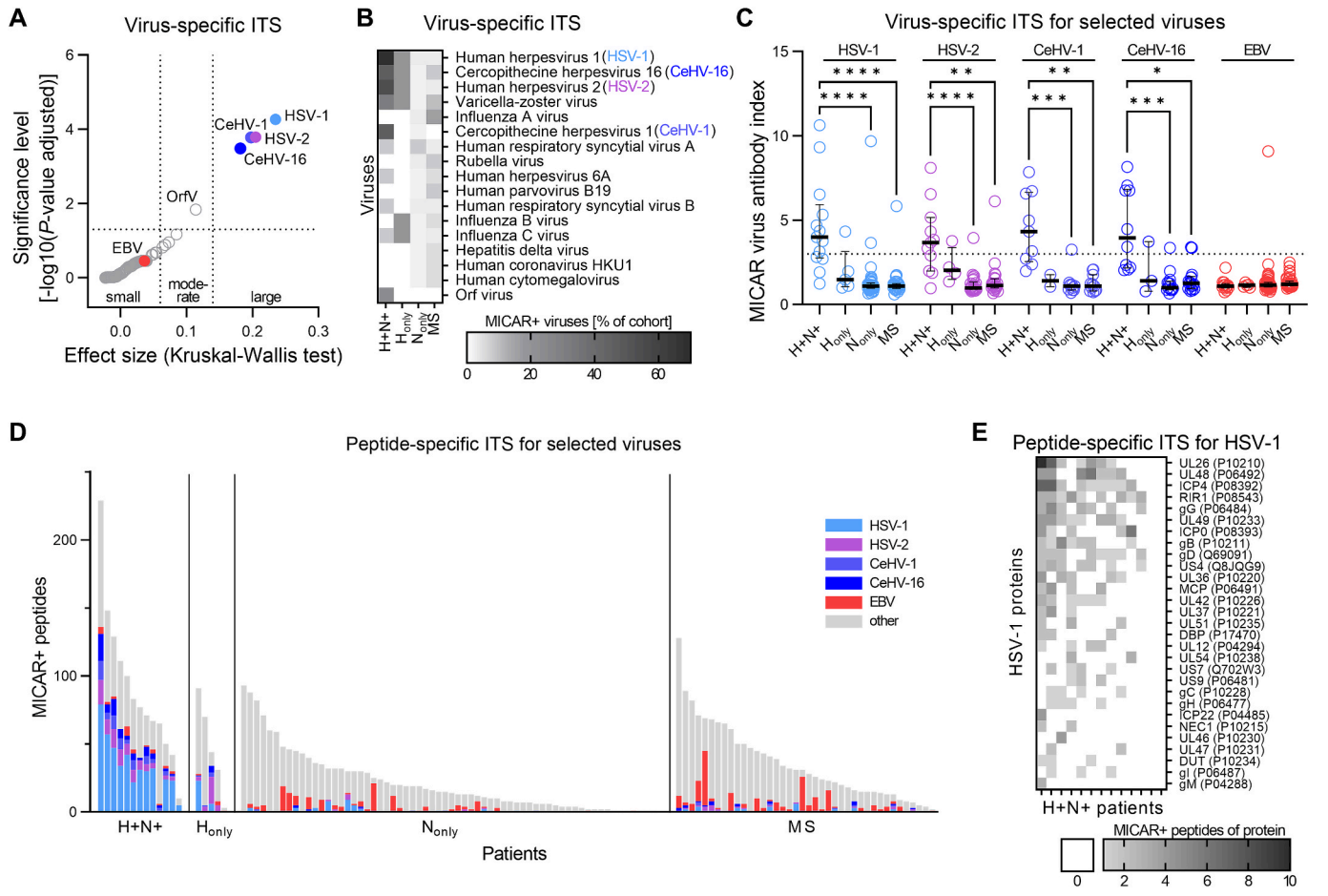

Fig. 3. MICAR elucidates intrathecal HSV antibodies. (A) Effect sizes and significance levels of Kruskal-Wallis tests are shown from comparison of MICAR virus antibody indices between disease cohorts (n = 123 paired CSF/serum samples). Viruses for which > 1 MICAR index was computed (n = 109) are shown. Dotted lines indicate thresholds for effect size (Statistical Power Analysis for the Behavioral-Sciences, 1988) and statistical significance (P-values adjusted using Benjamini-Hochberg procedure). (B) A heat map illustrates relative frequencies of positive MICAR virus antibody indices (n = 123 paired CSF/serum samples). All viruses with > 1 MICAR index in any disease cohort are shown and ordered by total count of MICAR+ indices. (C) Scattered dot plots display MICAR virus antibody indices for selected viruses (n = 123 paired CSF/serum samples). Black bars indicate the median with interquartile range. For comparison, Kruskal-Wallis test post-hoc multiple comparisons with Dunn's test were performed. The dotted line indicates positivity threshold. (D) Stacked bars represent counts of MICAR+ peptides (indicating peptide-specific ITS) from viral peptides from the VirScan PhIP-Seq library (n = 110,215). n = 123 paired CSF/serum samples. Selected viruses are highlighted by color and individuals ordered by the total counts of MICAR+ peptides within each disease cohort. (E) A heat map illustrates absolute frequencies of positive peptide-specific ITS by selected HSV-1 proteins and separately for all individuals of the H+N+ disease cohort (n = 13). All proteins of the HSV-1 proteome represented in the VirScan PhIP-Seq library (n = 46) with > 2 MICAR peptide antibody indices are shown. Data is ordered by total count of MICAR+ indices per protein (rows) and per individual (column).

antibody indices for HSVs and related monkey cercopithecine herpes viruses (CeHV) 1 and 16. In contrast, MICAR virus indices were rarely positive for other viruses (Fig. S4C-D), suggesting that the MICAR approach can detect even subtle antigen-specific ITS reliably and in a completely unbiased manner.

Comparing MICAR virus antibody indices between the four disease cohorts revealed significant differences, most prominently for HSVs and CeHVs (Fig. 3A), which were frequently positive in the H+N+, to a lesser extent in the H_{only}, and rarely in the N_{only} or MS cohorts (Fig. 3B-C). HSV-1 MICAR indices strongly correlated with those for HSV-2 and related CeHVs, likely due to antibody cross-reactivity (Fig. S4E-H). When examining the peptide reactivity levels, we identified that MICAR+ antibodies in the H+N+ cohort bound most frequently to HSV-1, and relatively less to HSV-2 or CeHV targets (Fig. 3D). Interestingly, while these intrathecal antibodies bound to a variety of proteins of the HSV-1 proteome, binding to UL26 and UL48 was most common (Fig. 3E).

3.3. *Enhanced antibody response to distinct HSV peptides is associated with post-HSE NMDARE*

With the established MICAR approach, we next sought to define differences in the antibody responses to HSV proteomes in HSE patients with NMDARE (H+N+) versus those that did not develop NMDARE (H_{only}). The samples of both cohorts were collected at comparable median time points (Fig. 4A) and revealed continuous detection of HSV antibodies even years after HSE, when acute signs of inflammation had vanished (Fig. S5A-B). The diversity of HSV antibodies in the CSF, i.e. the breadth of the antibody response, was similar in both cohorts (Fig. 4B). In some H_{only} samples the CSF antibodies targeted more HSV-1, in others more HSV-2 peptides, whereas in all H+N+ samples the CSF antibodies predominantly targeted HSV-1 peptides (Fig. 4C). Consistently, H+N+ patients displayed enhanced antibody responses towards HSV with greater antibody reactivity levels in the CSF and increased intrathecal antibody production (by counts of MICAR+ peptides); neither of the observations pertained to HSV-2 (Fig. 4D-E). When comparing binding patterns to the HSV proteome between the H+N+

and the H_{only} cohorts, we identified increased antibody binding to 23 HSV-1 peptides and one HSV-2 peptide and higher MICAR antibody indices for three HSV-1 peptides and one HSV-2 peptide in H+N+ patients, but none that are significantly enriched in the H_{only} cohort (Fig. 4F, Fig. S5C, Table S2, Table S3). For five HSV-1 peptides and one HSV-2 peptide, the antibody binding in the H+N+ cohort was more prevalent when compared to H_{only}, and also when compared to the non-HSE patients (N_{only} and MS cohorts), resulting in positive predictive values (PPV) $\geq$ 75% under both comparison conditions (Fig. 4G, Table S2). Interestingly, these six "signature peptides" belong to two proteins: the DNA polymerase processivity factor (gene UL42, three consecutive HSV-1 peptides) and the tegument protein VP16 (gene UL48, two consecutive HSV-1 peptides and one corresponding HSV-2 peptide with > 82% sequence homology to the respective HSV-1 UL48 sequence, Fig. S6A). Antibodies against one UL42 signature peptide (amino acids position 449 to 488), but not against any other of the H+N+ associated peptides, correlated with NMDAR-IgG titers (Fig. S6B-F). Using MEME software, we systematically searched for sequence homologies between HSV-1 UL42, HSV-1 UL48, and the human NMDAR which might explain the link between the signature peptides and the associated anti-neuronal autoimmunity. However, we found no significant motifs that are shared between the two HSV proteins or between the HSV proteins and the human receptor. Moreover, binding to PhIP-Seq HuScan library peptides representing the NR1 subunit of the NMDAR was not detected in any of the NMDARE patients. Both provide no support for molecular mimicry based on linear epitopes.

While each of the signature peptides had a specificity > 98%, the corresponding sensitivities to detect H+N+ patients were moderate, varying between 41% and 58% (Table S2). We observed that while some H+N+ patients responded to all signature peptides, others reacted only to subsets with varying patterns of distributions, and four patients displayed no reactivity at all (Fig. 4H). Hence, we incorporated the reactivity levels of the three HSV-1 UL42 and the two HSV-1 UL48 signature peptide antibodies into a combined UL42-UL48-antibody score (Fig. 4I).

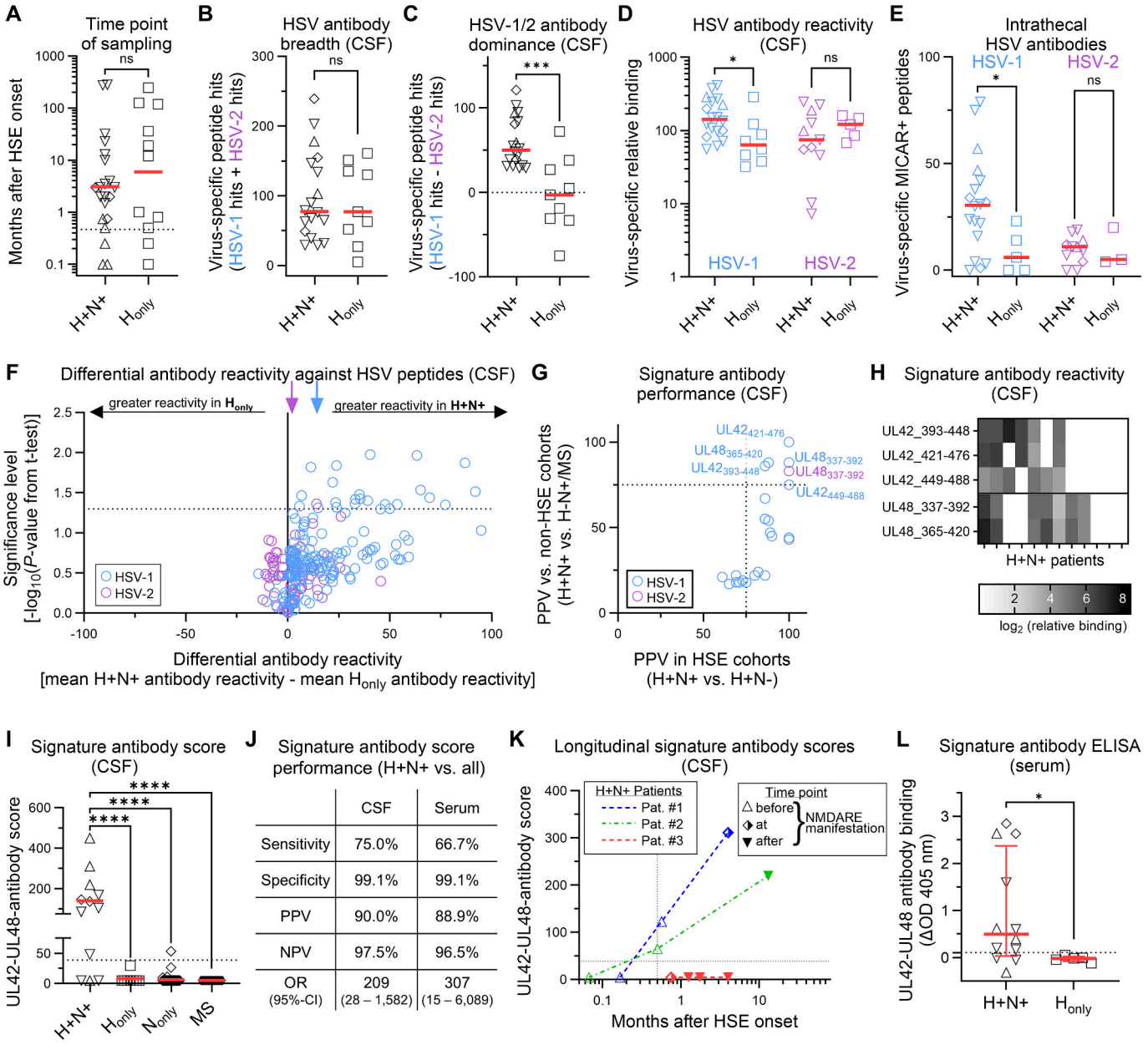

(caption on next page)

Fig. 4. Enhanced HSV antibody response to distinct peptides associates with NMDARE post-HSE. (A) Scattered dot plots display time points of sampling separately for each disease cohort (n = 21 samples from 13 H+N + individuals, n = 11 samples from 10 H_{only} individuals). For comparison, a Mann-Whitney test was performed. Red bars indicate geometric mean. Dotted line indicates the > 14 days cut-off that accounts for the antibody response after infection and was used for analyses shown in B-K. (B) Scattered dot plots display CSF antibody breadth (n = 18 samples from 12 H+N+ individuals, n = 9 samples from 8 H_{only} individuals). Red bars indicate median. For comparison, a Mann-Whitney test was performed. (C) Scattered dot plots display CSF HSV-1 versus HSV-2 antibody dominance (difference of HSV-1 and HSV-2 peptide hits, with values > 0 indicating greater breadth against HSV-1, and values < 0 indicating greater breadth against HSV-2). Same samples as in B. Red bars indicate median. For comparison, a Mann-Whitney test was performed. (D) Scattered dot plots display virus-specific antibody reactivity. Samples are only shown if antibody response to the respective virus is present in CSF. Same samples as in B. Red bars indicate median. For comparison, Mann-Whitney tests were performed. (E) Scattered dot plots display virus-specific intrathecal antibodies. Same samples as in B, shown if antibody response to the respective virus is present in CSF. Red bars indicate median. For comparison, Mann-Whitney tests were performed. (F) A volcano plot illustrating differential reactivity patterns of HSV peptide targets, compared between CSF antibodies from H+N+ (n = 12) and H_{only} (n = 8) individuals. HSV-1 (n = 216) and HSV-2 (n = 89) peptides are shown if detected in at least one H+N+ or H_{only} individual. For comparison of mean reactivities between cohorts, two-tailed t-tests were performed. Positive differential antibody reactivity (right side) indicates greater mean reactivity in H+N+ cohort, negative values (left side) greater mean reactivity in H_{only} cohort. Arrows above graph indicate mean of antibody reactivity for all peptides representing HSV-1 (blue) and HSV-2 (purple). Dotted lines indicate threshold for statistical significance based on unadjusted P-values. (G) Positive predictive values (PPV) for HSV-1 and HSV-2 peptides with differential CSF antibody reactivity in H+N+ versus H_{only} disease cohorts (derived from C) are shown. PPVs are shown for identification of H+N+ versus H_{only} cohort (x-axis) and versus non-HSE cohorts (y-axis). For peptides with PPVs ≥ 75% (dotted lines) under both comparison conditions, the HSV protein and the amino acid positions within the protein are shown. (H) A heat map illustrates CSF antibody reactivities for five HSV-1 signature peptides (n = 12 H+N+ individuals). (I) Scattered dot plots display UL42-UL48-antibody scores (n = 128 CSF samples). Red bars indicate median. For comparison, Kruskal-Wallis tests were performed with post-hoc multiple comparisons using Dunn's test. Dotted line indicate threshold of positivity of 38.8. (J) Parameters of UL42-UL48-antibody score test performance are shown (128 CSF and 124 serum samples of entire study cohort). Thresholds of positivity defined at 38.8 for CSF and 15.3 for serum samples (Methods). (K) Plot shows longitudinal UL42-UL48-antibody score for 3 H+N+ individuals with available longitudinal CSF measurements. The vertical dotted line indicates > 14 days cut-off that accounts for the antibody response after infection and was used for analyses shown in B-K. The horizontal dotted line indicates threshold of positivity of 38.8. (L) Scattered dot plots display antibody binding to five signature peptides (as in H) from ELISA measurements with n = 12 H+N+ individuals and n = 5 H_{only} individuals. Optical density (OD) measurements are median from three independent experiments and are shown after subtraction of sample-specific OD from control wells without preincubation with the signature peptides. For comparison, a Mann-Whitney test was performed. Red bars indicate median + interquartile range. For the H+N+ cohort, upward-point arrowheads represent samples before NMDARE was diagnosed, diamonds represent samples at time of NMDARE manifestation, and downward-point arrowheads represent samples after NMDARE manifestation. CI = confidence interval. NPV = negative predictive value, ns = not significant, PPV = positive predictive value. (For interpretation of the references to color in this figure legend, the reader is referred to the web version of this article.)

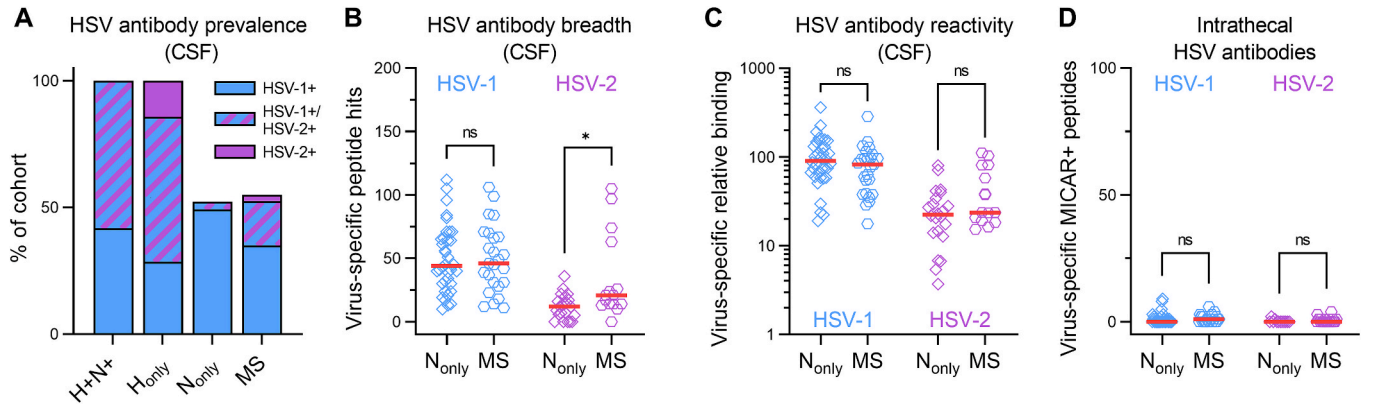

Fig. 5. No link between HSV immunity and NMDARE patients without a history of HSE. (A) Bar plots display prevalence of CSF antibody responses to HSV-1 and HSV-2 (n = 128 CSF samples) for all disease cohorts. Prevalence of antibody reactivity is defined by VAR scores > 0.72 (Methods). (B) Scattered dot plots display CSF antibody breadth against HSV-1 and HSV-2 for N_{only} and MS cohort. Samples are only shown, if antibody response to respective virus is present in patient's CSF or serum (N_{only}: 36 HSV-1, 22 HSV-2, MS: 25 HSV-1, 15 HSV-2). Red bars indicate median. For comparison, Mann-Whitney tests were performed. (C) Scattered dot plots display virus-specific antibody reactivity against HSV-1 and HSV-2. Same samples as in B. Red bars indicate median. For comparison, Mann-Whitney tests were performed. Scale on y-axis as in Fig. 4D for better comparison. (D) Scattered dot plots display virus-specific intrathecal antibodies against HSV-1 and HSV-2. Same samples as in B. Red bars indicate median. For comparison, Mann-Whitney tests were performed. Scales on y-axis as in Fig. 4E for better comparison. (For interpretation of the references to color in this figure legend, the reader is referred to the web version of this article.)

It is important to emphasize that the UL42-UL48-antibody score aggregates reactivities only against the five signature peptides, not against the entire UL42 and UL48 proteins, as reactivities against non-signature peptides of these proteins were more similar across all four disease cohorts (Fig. S6G-H).

Applying the UL42-UL48-antibody score to the entire study cohort, resulted in an increased sensitivity of 75% in CSF (>66% in serum) and a robust specificity > 99%, both within the entire study cohort and within the HSE cohorts (Fig. 4I-J, Fig. S7A). A positive score in the CSF was associated with an OR of 46 (CI 2 – 1,029) for distinguishing H+N+ from H_{only} individuals, and an OR of 209 (28 – 1,582) for distinguishing H+N+ from all other individuals in our study population, with similar values observed in serum (Fig. 4J). We found robust stability of UL42-UL48-antibody score measurements in longitudinal samples (Fig. S7B) and identified positive score in H+N+ samples taken before, at, and after manifestation of NMDARE (Fig. S7C). Of three H+N+ patients with available longitudinal CSF samples, all had negative UL42-UL48-antibody scores at the initial sampling, suggesting that the signature antibodies were not pre-existing before HSE. In two of these patients, UL42-UL48-antibody scores were highly positive at the last available sampling (after NMDARE manifestation). Notably, in both cases, the signature antibodies were already detectable in samples taken 2–3 weeks after HSE onset, but prior to clinical NMDARE diagnosis (Fig. 4K). Finally, we orthogonally validated the UL42-UL48-antibody score using an ELISA with the five signature peptides. Sera from 75% of H+N+ individuals, but none from the H-only group, showed signals above the

cut-off (Fig. 4L), demonstrating concordance with the PhIP-Seq results (Fig. S7D).

Collectively, this suggests that these signature antibodies can distinguish H+N+ from H_{only} and non-HSE patients and may have potential to predict NMDARE development in post-HSE patients.

3.4. HSV antibodies are not associated with NMDARE in patients without a history of HSE

Since some reports have suggested (Nosadini et al., 2017; Salovin et al., 2018) a link between HSV immunity and NMDARE even in patients without prior HSE, we compared HSV antibody responses between the non-HSE cohorts (N_{only} and MS). First, by prevalence, we detected HSV antibodies in approximately half of N_{only} patients, both in CSF (52%, Fig. 5A) and in serum samples (55%, Fig. S8A), similar to MS patients (55%, 63%). Second, by quantity, we found similar characteristics of HSV antibody responses in the two cohorts (N_{only} and MS). There was no single parameter significantly increased in the N_{only} cohort, neither for HSV-1 nor for HSV-2, when comparing the diversity of HSV antibody targets in CSF (Fig. 5B) or in serum (Fig. S8B), the level of antibody reactivity in CSF (Fig. 5C) or in serum (Fig. S8C), and the count of intrathecal antibodies (Fig. 5D, Fig. 3B-C). Third, by quality, in a systematic comparison of HSV binding patterns, we identified only a single peptide with increased antibody binding in the N_{only} versus the MS cohort (Fig. S8D), however, with poor performance to differentiate between the two cohorts (Table S4). Collectively, these findings indicate that the link between HSV immunity and NMDAR autoimmunity is likely limited to the post-HSE condition.

4. Discussion

In this study, we addressed the medical need for biomarkers to identify HSE patients at risk for secondary NMDARE. We analyzed antibody reactome profiles against all human viruses and introduce a novel metric to quantify intrathecal antibody reactivities. We identified a distinctive antibody signature associated with NMDARE development, which may in the future enable early intervention to reduce disease burden from secondary autoimmunity.

4.1. Functions of UL42 and UL48 proteins and antibodies

Recent investigations in a prospective HSE cohort had observed increased blood type I interferon responses 21 days after HSE onset in 20% of patients that went on to develop secondary autoimmune encephalitis (Armangue et al., 2023). This slower decay of interferon activation indicates a prolonged viral immune response (Leib, 2002; Mesev et al., 2019), which is associated with increased antibody production (Le Bon et al., 2001). In the present study, we could not assess this interferon signature due to the lack of suitable biospecimens. However, we found distinctive features in the HSV antibody responses in the H+N+ compared to the H_{only} cohort that are consistent with a prolonged HSV response. First, HSV antibodies of all H+N+ individuals preferentially bound HSV-1 over HSV-2 targets, suggesting an infection with HSV-1, which is consistent with PCR results showing that H+N+ cases are predominantly preceded by HSV-1 infections (Armangue et al., 2023). Second, the total HSV-1, but not HSV-2, antibodies showed greater level of reactivity and were more frequently a result of ITS. Third, the enhanced HSV-1 response in H+N+ individuals comprised a differential pattern of HSV-1 antibody reactivities. The differential reactivity pattern was more related to differences in specific peptides targeted, versus differences in peptide-specific ITS. This H+N+ associated antibody reactivity pattern comprised five distinct peptides from the HSV-1 UL42 and UL48 proteins. By sequence analysis between UL42, UL48 and the NMDAR, we did not find any evidence for molecular mimicry based on linear epitopes, as previously supposed by some authors (Nosadini et al., 2017; Salovin et al., 2018). Given that the signature peptides are derived from two different HSV-1 proteins and that H+N+ patients contained signature antibodies in varying distributions, it is also unlikely that molecular mimicry of conformational epitopes can explain the association to NMDAR autoimmunity. Perhaps more likely is that UL42 and UL48 antibodies are associated with enhanced inflammatory responses that subsequently break tolerance to the NMDAR autoantigen. Interestingly, both UL42 and UL48 proteins, despite divergent role in viral life cycle, inhibit NF-κB activation (Chapon et al., 2019; Xing et al., 2013; Zhang et al., 2013), and thus abrogate the production of type I interferons (Le Bon et al., 2001; Pfeffer, 2011). If the UL42 and UL48 antibodies are able to reach their intracellular targets (Pinal-Fernandez et al., 2024; Rocchi et al., 2019), it is conceivable that they could disinhibit this HSV-1-protein mediated interferon suppression, thereby providing a potential mechanism for immune hyperactivation (and ensuing autoantibody development), similar to what has been proposed in anti-MDA5 dermatomyositis (Pinal-Fernandez et al., 2020, 2024; Jayaraman et al., 2025). Alternatively, such antibodies targeting interferon-binding proteins may promote the development of interferon autoantibodies through epitope spreading, potentially modulating the immune response. Via these two or some other pathways, antibodies to different epitopes of UL42 and UL48 may differentially dysregulate interferon signaling, potentially explaining why some, but not all, UL42 and UL48 antibodies are associated with secondary NMDARE. Interestingly, HSV-1 UL48 antibodies were previously described in 30% of Behçet's disease patients (Zheng et al., 2015), an autoimmune systemic vasculitis, consistent with a role in activation of (auto)immunity.

4.2. Potential diagnostic utility of HSV-1 signature antibodies in HSE patients

While these signature antibodies were frequent in H+N+ individuals, they were found only in two of 70 NMDARE patients without a history of HSE. This is consistent with a link between NMDARE and HSV infections (Armangue et al., 2018; Pruss et al., 2012) that applies exclusively to post-HSE cases. A previous study had reported a significantly increased HSV-1 prevalence in their non-HSE-encephalitis NMDARE cohort (n = 39) at 49% (Salovin et al., 2018), which however might be due to the unusually low 21% prevalence of HSV-1 seropositivity among that study's controls (Bradley et al., 2014; Chemaitelly et al., 2019; James et al., 2020). In contrast, our study's larger N_{only} cohort (n = 70) demonstrated HSV antibody responses with no evidence of enhanced reactivities and with a prevalence of ~ 50%, similar to the MS control cohort and within the typical range of Western populations (Bradley et al., 2014; Chemaitelly et al., 2019; James et al., 2020). Interestingly, in the clinical records of the one N_{only} individual with low-level detection of signature antibodies, we found that HSV-specific ITS was detected as part of the clinical diagnostics from an earlier CSF/serum pair (3 weeks after NMDARE onset, no material left for this study). The HSV-specific ITS may indirectly reflect an HSE despite negative HSV-PCR, which can occur if too few viral particles are in the CSF at the time point of lumbar puncture (de Montmollin et al., 2022). Since the question of HSE could not be fully clarified, we considered this case to be N_{only}. If it had been excluded, the specificity and PPV of the UL42-UL48-antibody score would have been further increased to 100% for CSF from 128 individuals tested in this study.

Independently, the UL42-UL48-antibody score revealed high sensitivity for H+N+ individuals (9/12 in CSF, 8/12 in serum), and was rarely positive in the other cohorts (H_{only}: 0/8 in CSF, 0/5 in serum; non-HSE groups: 1/108 in CSF, 1/107 in serum). Importantly, within the H+N+ cohort, signature antibodies were detected before and after NMDARE manifestation, supporting their potential use as a prognostic biomarker in HSE to evaluate the risk for secondary NMDARE. As HSE can result from primary HSV infection or from HSV reactivation (Ak et al., 2024; Steiner, 2011), clinical utilization in the context of primary infection will have to consider that seroconversion requires

approximately two weeks (Ashley et al., 1999), which is typically before the onset of NMDARE (with median delay of 39 days after HSE) (Armangue et al., 2023). Once induced, signature antibodies will likely be detectable over a long period of time, given the remarkable stability of IgG responses (Amanna et al., 2007) and their detection in some of our cohort's H+N+ individuals in up to > 20 years after HSE. Collectively, this suggests the utility of UL42 and UL48 signature antibodies as a biomarker for risk of NMDARE after HSE. Future studies should validate these findings in independent HSE cohorts, investigate the potential influence of different HSV-1 and HSV-2 strains, and potentially explore additional orthogonal antibody detection assays. They should preferentially compare samples at different time points at and after HSE onset and evaluate the influence of concurrent steroid treatment in HSE treatment (Whitfield et al., 2021). If validated, predictive signature antibody detection in HSE patients could enable early stratification of risk for secondary NMDARE and guide clinical decision making, similar to lupus anticoagulant and anti-ribosomal P antibodies that are predictive for neuropsychiatric events in systemic lupus erythematosus patients (Hanly et al., 2011). For HSE patients with high-risk for NMDARE, more frequent clinical follow-ups and NMDAR autoantibody testing (particularly from CSF) may reduce diagnosis delays for secondary NMDARE. Ultimately, earlier initiation of immunosuppressive therapies (possibly in selected cases even before the detection of NMDAR autoantibodies) may reduce long-term morbidity from post-HSE autoimmunity or even prevent its onset, similar to benefits from early treatment initiation in other neuroimmunological conditions such as MS (Cobo-Calvo et al., 2023; Harding et al., 2019; He et al., 2020) or NMDARE independent of previous HSE (Titulaer et al., 2013). Moreover, future experimental studies should aim to isolate signature antibodies (Kreye et al., 2016; Kreye et al., 2021) to discern their bioactivity in vitro and in vivo.

4.3. Limitations

This study has several limitations. First, the number of patients is relatively low, especially in the H+N+ cohort, given the rare nature of this condition. The age of the H+N+ patients investigated here (median 64 years) was higher than in other cohorts (34 years, Armangue et al., 2023) and thereby underrepresents children. Second, the samples were collected in a multicenter study at heterogenous and non-standardized time points. While variability in sampling time could, in principle, influence antibody detection, IgG responses are generally persistent (Amanna et al., 2007; Vogl et al., 2021), also notable in our cohort (Fig. S5B), which likely mitigates any effect of minor differential sampling times. Third, due to limited sample volumes, we focused on retesting NMDAR autoantibodies only (Fig. S1) and did not conduct broader CBA screening. Thus, H_{only} individuals were classified based on at least 3 months of follow-up without clinical suspicion of secondary autoimmune encephalitis. We cannot rule out transient post-HSE autoantibody development, but without relevant symptoms, these cases do not meet criteria for autoimmune encephalitis per current guidelines (Graus et al., 2016). Fourth, we did not have access to samples before HSE onset. In some individuals, pre-existing HSV antibody responses, such as those from prior infections, may have influenced our results. In two H+N+ individuals we observed that signature antibodies were induced by HSE, but we could not systematically investigate whether they can be pre-existing before HSE. And last, despite detailed profiling of antibody responses to the HSV proteome, our analyses may have overlooked HSV antibodies to targets that are not captured in the PhIP-Seq library which are restricted to 56-mer peptide tiles and HSV sequences published at the time of its design (Xu et al., 2015).

4.4. Conclusion and perspective on MICAR applications

In conclusion, we present distinct features of an enhanced HSV antibody response associated with NMDARE development in HSE patients and report an antibody biomarker signature with potential utility for risk stratification. In our study cohort, we found no heightened or differential HSV antibody reactivities in NMDARE patients without a history of HSE. These unbiased analyses of the intrathecal antibody reactome are made possible via the MICAR metric, developed and reported here. MICAR uses multiplexed evaluation of antibody compartment-specificity and can analyze ITS at the level of total IgG, virus specificity, and peptide specificity. In this first application of MICAR, we found HSV-specific ITS years after HSE and even below the clinical threshold for ITS of total IgG. Given the relevance of target-specific ITS for infectious and autoimmune diseases of the CNS (Pruss, 2021; Rodriguez-Mogeda et al., 2024; Shamier et al., 2021; Thompson et al., 2018) and MICAR's unbiased nature to identify ITS targets, MICAR will advance future investigations in neuroimmunology and support the discovery of novel immune targets, immunological disease associations, and antibody cross-reactivities. While we solely demonstrate MICAR's utility with PhIP-Seq data, the approach could readily be adapted to other multiplexed antibody assay types, including protein and peptide arrays (Jeong et al., 2012; Sjoberg et al., 2016), yeast display platforms (Wang et al., 2022), and human cell display systems (Freeth and Soden, 2020; Tucker et al., 2018). Further, beyond investigating CSF-specific antibodies as ITS, MICAR may also find utility in characterizing antibodies specific to other body fluids (e.g. from the pulmonary system, gastrointestinal tract, or synovial fluid) (Fekkar et al., 2008), or specific to tissues, including from biopsies and tumor resections.

CRediT authorship contribution statement

Jakob Kreye: Writing – review & editing, Writing – original draft, Visualization, Validation, Supervision, Software, Resources, Project administration, Investigation, Funding acquisition, Formal analysis, Data curation, Conceptualization. **William R. Morgenlander:** Writing – review & editing, Methodology, Formal analysis, Data curation. **Manjusha Thakar:** Writing – review & editing, Methodology, Investigation, Formal analysis. **Poul M. Schulte-Frankenfeld:** Writing – review & editing, Visualization, Formal analysis. **Sarah Schott:** Formal analysis, Investigation, Writing – review & editing. **Isabel Bünger:** Formal analysis, Investigation, Writing – review & editing. **Hans-Christian Kornau:** Writing – review & editing, Funding acquisition, Formal analysis. **Julia W. Angkeow:** Writing – review & editing, Methodology, Formal analysis. **Sahana Jayaraman:** Writing – review & editing, Methodology, Formal analysis. **Carolin Otto:** Writing – review & editing, Resources. **Wiebke Hahn:** Writing – review & editing, Resources. **Jan Lewerenz:** Writing – review & editing, Resources. **Franziska S. Thaler:** Writing – review & editing, Resources. **Mirjam Korporal-Kuhnke:** Writing – review & editing, Resources. **Nico Melzer:** Writing – review & editing, Resources. **Justina Dargvainiene:** Writing – review & editing, Resources. **Christian G. Bien:** Writing – review & editing, Resources. **Rose Kohlie:** Writing – review & editing, Investigation. **Erik Lattwein:** Writing – review & editing, Investigation. **Dietmar Schmitz:** Writing – review & editing, Resources. **Peter A. Calabresi:** Writing – review & editing, Resources. **Carlos A. Pardo:** Writing – review & editing, Resources, Funding acquisition. **Harald Prüss:** Writing – review & editing, Resources, Funding acquisition. **Klemens Ruprecht:** Writing – review & editing, Resources. **H. Benjamin Larman:** Writing – review & editing, Writing – original draft, Supervision, Methodology, Funding acquisition, Conceptualization.

Ethics approval

All patients or their legal representatives gave their informed consent prior to participation. The study was approved by the Ethics Review Committee at Charité – Universitätsmedizin Berlin, corporate member of Freie Universität Berlin and Humboldt-Universität zu Berlin, Berlin, Germany (ethical vote number EA4/046/23).

Funding

Related to this work, J.K. has received a Fulbright Scholar grant by the German-American Fulbright Commission and a Clinician Scientist fellowship by the Berlin Institute of Health at Charité. This work was supported by the German Federal Ministry of Education and Research (research association grant CONNECT-GENERATE, 01GM1908A, 01GM1908C, 01GM1908D, 16GW0279K, 01GM2208A and 01GM2208C)), by the German Research Council DFG (FOR3004, project number 415914819: KR5870/1-1 to J.K., KO 2290/3-2 to H.-C.K., PR1274/9-1 to H.P. and clinical research unit 5023/1 'BECAUSE-Y' to H.P.), by the Helmholtz Association (HIL-A03 to H.P.), and by National Institutes of Health grants (R01 GM136724 to H.B.L., R01 NS110112 and R01 NS123712 to C.A.P.).

Declaration of competing interest

The authors declare the following financial interests/personal relationships which may be considered as potential competing interests: A patent application related to this work has been filed (European Patent Application No. 24187247.2: 'Biomarkers for Herpes-simplex virus autoimmunity') with J.K. and H.B.L. named as inventors. M.K.K. received speaker's honoraria from Novartis, BMS and Merck. P.A.C. is a PI on a grant from Genentech to JHU, and has received consulting fees from Lilly and Project Efflux. K.R. received research support from Novartis, Merck Serono, European Union (821283–2), Arthur Arnstein Foundation and speaker's honoraria from Virion Serion and Novartis. R. K. and E.L. are employees of EUROIMMUN, a company that manufactures diagnostic tests and instruments. R.K. and E.L. did not benefit from any potential or actual financial gain as a result of the work. H.B.L. is an inventor on an issued patent (US20160320406A) filed by Brigham and Women's Hospital that covers the VirScan technology. H.B.L. is a co-founder of Infinity Bio, Portal Bioscience, and Alchemab Therapeutics. The authors have no additional financial interests.

Acknowledgements

The authors acknowledge the Central Biobank Charité (ZeBanC) for samples and data, used in this study. The authors are grateful to Stephen Elledge, PhD, for providing the VirScan and human proteome PhIP-Seq libraries. The graphical abstract was created in BioRender.

Appendix A. Supplementary data

Supplementary data to this article can be found online at https://doi.org/10.1016/j.bbi.2025.106073.

Data availability

The authors confirm all relevant data supporting the key findings of this study are available within the article and its supplementary data. Derived data required to reanalyze the reported findings of this study are available from the corresponding authors upon request.

References

Statistical Power Analysis for the Behavioral-Sciences, 1988. Statistical power analysis for the behavioral-sciences - cohen. J. Percept Motor Skill 67, 1007.

Ak, A.K., Bhutta, B.S., Mendez, M.D., 2024. Herpes Simplex Encephalitis. StatPearls, Treasure Island (FL).

Amanna, I.J., Carlson, N.E., Slifka, M.K., 2007. Duration of humoral immunity to common viral and vaccine antigens. N. Engl. J. Med. 357, 1903–1915. https://doi.org/10.1056/NEJMoa066092.

Andersson, M., Alvarez-Cermeno, J., Bernardi, G., Cogato, I., Fredman, P., Frederiksen, J., Fredrikson, S., Gallo, P., Grimaldi, L.M., Gronning, M., et al., 1994. Cerebrospinal fluid in the diagnosis of multiple sclerosis: a consensus report. J. Neurol. Neurosurg. Psychiatry 57, 897–902. https://doi.org/10.1136/jnnp.57.8.897.

Angkeow, J.W., Monaco, D.R., Chen, A., Venkataraman, T., Jayaraman, S., Valencia, C., Sie, B.M., Liechti, T., Farhadi, P.N., Funez-dePagnier, G., Sherman-Baust, C.A., Wong, M.Q., Ruczinski, I., Caturegli, P., Sears, C.L., Simner, P.J., Round, J.L., Duggal, P., Laserson, U., Steiner, T.S., Sen, R., Lloyd, T.E., Roederer, M., Mammen, A.L., Longman, R.S., Rider, L.G., Larman, H.B., 2022. Phage display of environmental protein toxins and virulence factors reveals the prevalence, persistence, and genetics of antibody responses. Immunity 55 (1051–1066), e1054.

Armangue, T., Moris, G., Cantarin-Extremera, V., Conde, C.E., Rostasy, K., Erro, M.E., Portilla-Cuenca, J.C., Turon-Vinas, E., Malaga, I., Munoz-Cabello, B., Torres-Torres, C., Llufriu, S., Gonzalez-Gutierrez-Solana, L., Gonzalez, G., Casado-Naranjo, I., Rosenfeld, M., Graus, F., Dalmau, J., 2015. Autoimmune post-herpes simplex encephalitis of adults and teenagers. Neurology 85, 1736–1743. https://doi.org/10.1212/WNL.0000000000002125.

Armangue, T., Olive-Cirera, G., Martinez-Hernandez, E., Rodes, M., Peris-Sempere, V., Guasp, M., Ruiz, R., Palou, E., Gonzalez, A., Marcos, M.A., Erro, M.E., Bataller, L., Corral-Corral, I., Planaguma, J., Caballero, E., Vlagea, A., Chen, J., Bastard, P., Materna, M., Marchal, A., Abel, L., Cobat, A., Alsina, L., Fortuny, C., Saiz, A., Mignot, E., Vanderver, A., Casanova, J.L., Zhang, S.Y., Dalmau, J., 2023. Neurologic complications in herpes simplex encephalitis: clinical, immunological and genetic studies. Brain 146, 4306–4319. https://doi.org/10.1093/brain/awad238.

Armangue, T., Spatola, M., Vlagea, A., Mattozzi, S., Carceles-Cordon, M., Martinez-Heras, E., Llufriu, S., Muchart, J., Erro, M.E., Abraira, L., Moris, G., Monros-Gimenez, L., Corral-Corral, I., Montejo, C., Toledo, M., Bataller, L., Secondi, G., Arino, H., Martinez-Hernandez, E., Juan, M., Marcos, M.A., Alsina, L., Saiz, A., Rosenfeld, M.R., Graus, F., Dalmau, J., 2018. Frequency, symptoms, risk factors, and outcomes of autoimmune encephalitis after herpes simplex encephalitis: a prospective observational study and retrospective analysis. Lancet Neurol. 17, 760–772. https://doi.org/10.1016/S1474-4422(18)30244-8.

Ashley, R.L., Eagleton, M., Pfeiffer, N., 1999. Ability of a rapid serology test to detect seroconversion to herpes simplex virus type 2 glycoprotein G soon after infection. J. Clin. Microbiol. 37, 1632–1633. https://doi.org/10.1128/JCM.37.5.1632-1633.1999.

Bailey, T.L., Elkan, C., 1994. Fitting a mixture model by expectation maximization to discover motifs in biopolymers. Proc. Int. Conf. Intell. Syst. Mol. Biol. 2, 28–36.

Bailey, T.L., Johnson, J., Grant, C.E., Noble, W.S., 2015. The MEME Suite. Nucleic Acids Res. 43, W39–W49. https://doi.org/10.1093/nar/gkv416.

Bradley, H., Markowitz, L.E., Gibson, T., McQuillan, G.M., 2014. Seroprevalence of herpes simplex virus types 1 and 2–United States, 1999–2010. J. Infect Dis. 209, 325–333. https://doi.org/10.1093/infdis/jit458.

Bradshaw, M.J., Venkatesan, A., 2016. Herpes simplex virus-1 encephalitis in adults: pathophysiology, diagnosis, and management. Neurotherapeutics 13, 493–508. https://doi.org/10.1007/s13311-016-0433-7.

Bunger, I., Talucci, I., Kreye, J., Holtje, M., Makridis, K.L., Foverskov Rasmussen, H., van Hoof, S., Cordero-Gomez, C., Ullrich, T., Sedlin, E., Kreissner, K.O., Hoffmann, C., Milovanovic, D., Turko, P., Paul, F., Meckies, J., Verlohren, S., Henrich, W., Chaoui, R., Maric, H.M., Kaindl, A.M., Pruss, H., 2023. Synapsin autoantibodies during pregnancy are associated with fetal abnormalities. Brain Behav. Immun. Health 33, 100678. https://doi.org/10.1016/j.bbih.2023.100678.

Ceanga, M., Rahmati, V., Haselmann, H., Schmidl, L., Hunter, D., Brauer, A.K., Liebscher, S., Kreye, J., Pruss, H., Groc, L., Hallermann, S., Dalmau, J., Ori, A., Heckmann, M., Geis, C., 2023. Human NMDAR autoantibodies disrupt excitatory-inhibitory balance, leading to hippocampal network hypersynchrony. Cell Rep. 42, 113166. https://doi.org/10.1016/j.celrep.2023.113166.

Chapon, M., Parvatiyar, K., Aliyari, S.R., Zhao, J.S., Cheng, G., 2019. Comprehensive mutagenesis of herpes simplex virus 1 genome identifies UL42 as an inhibitor of type I interferon induction. J. Virol. 93. https://doi.org/10.1128/JVI.01446-19.

Chemaitelly, H., Nagelkerke, N., Omori, R., Abu-Raddad, L.J., 2019. Characterizing herpes simplex virus type 1 and type 2 seroprevalence declines and epidemiological association in the United States. PLoS One 14, e0214151. https://doi.org/10.1371/journal.pone.0214151.

Cobo-Calvo, A., Tur, C., Otero-Romero, S., Carbonell-Mirabent, P., Ruiz, M., Pappolla, A., Villacieros Alvarez, J., Vidal-Jordana, A., Arrambide, G., Castillo, J., Galan, I., Rodriguez Barranco, M., Midaglia, L.S., Nos, C., Rodriguez Acevedo, B., Zabalza de Torres, A., Mongay, N., Rio, J., Comabella, M., Auger, C., Sastre-Garriga, J., Rovira, A., Tintore, M., Montalban, X., 2023. Association of very early treatment initiation with the risk of long-term disability in patients with a first demyelinating event. Neurology 101, e1280–e1292. https://doi.org/10.1212/WNL.0000000000207664.

Dahm, L., Ott, C., Steiner, J., Stepniak, B., Teegen, B., Saschenbrecker, S., Hammer, C., Borowski, K., Begemann, M., Lemke, S., Rentzsch, K., Probst, C., Martens, H., Wienands, J., Spalletta, G., Weissenborn, K., Stocker, W., Ehrenreich, H., 2014. Seroprevalence of autoantibodies against brain antigens in health and disease. Ann. Neurol. 76, 82–94. https://doi.org/10.1002/ana.24189.

Dalmau, J., Armangue, T., Planaguma, J., Radosevic, M., Mannara, F., Leypoldt, F., Geis, C., Lancaster, E., Titulaer, M.J., Rosenfeld, M.R., Graus, F., 2019. An update on anti-NMDA receptor encephalitis for neurologists and psychiatrists: mechanisms and models. Lancet Neurol. 18, 1045–1057. https://doi.org/10.1016/S1474-4422(19)30244-3.

Dalmau, J., Gleichman, A.J., Hughes, E.G., Rossi, J.E., Peng, X., Lai, M., Dessain, S.K., Rosenfeld, M.R., Balice-Gordon, R., Lynch, D.R., 2008. Anti-NMDA-receptor encephalitis: case series and analysis of the effects of antibodies. Lancet Neurol. 7, 1091–1098. https://doi.org/10.1016/S1474-4422(08)70224-2.

Dalmau, J., Graus, F., 2018. Antibody-mediated encephalitis. N. Engl. J. Med. 378, 840–851. https://doi.org/10.1056/NEJMra1708712.

Dalmau, J., Tuzun, E., Wu, H.Y., Masjuan, J., Rossi, J.E., Voloschin, A., Baehring, J.M., Shimazaki, H., Koide, R., King, D., Mason, W., Sansing, L.H., Dichter, M.A.,

Rosenfeld, M.R., Lynch, D.R., 2007. Paraneoplastic anti-N-methyl-D-aspartate receptor encephalitis associated with ovarian teratoma. Ann. Neurol. 61, 25–36. https://doi.org/10.1002/ana.21050.

de Montmollin, E., Dupuis, C., Jaquet, P., Sarton, B., Sazio, C., Susset, V., Conrad, M., Argaud, L., Demeret, S., Tadie, J.M., Barbier, F., Wolff, M., Timsit, J.F., Visseaux, B., Sonneville, R., 2022. Herpes simplex virus encephalitis with initial negative polymerase chain reaction in the cerebrospinal fluid: prevalence, associated factors, and clinical impact. Crit. Care Med. 50, e643–e648. https://doi.org/10.1097/CCM.0000000000005485.

Fekkar, A., Bodaghi, B., Touafek, F., Le Hoang, P., Mazier, D., Paris, L., 2008. Comparison of immunoblotting, calculation of the Goldmann-Witmer coefficient, and real-time PCR using aqueous humor samples for diagnosis of ocular toxoplasmosis. J. Clin. Microbiol. 46, 1965–1967. https://doi.org/10.1128/JCM.01900-07.

Freeth, J., Soden, J., 2020. New advances in cell microarray technology to expand applications in target deconvolution and off-target screening. SLAS Discov 25, 223–230. https://doi.org/10.1177/2472555219897567.

George, B.P., Schneider, E.B., Venkatesan, A., 2014. Encephalitis hospitalization rates and inpatient mortality in the United States, 2000-2010. PLoS One 9, e104169. https://doi.org/10.1371/journal.pone.0104169.

Graus, F., Titulaer, M.J., Balu, R., Benseler, S., Bien, C.G., Cellucci, T., Cortese, I., Dale, R. C., Gelfand, J.M., Geschwind, M., Glaser, C.A., Honnorat, J., Hoftberger, R., Iizuka, T., Irani, S.R., Lancaster, E., Leypoldt, F., Pruss, H., Rae-Grant, A., Reindl, M., Rosenfeld, M.R., Rostasy, K., Saiz, A., Venkatesan, A., Vincent, A., Wandinger, K.P., Waters, P., Dalmau, J., 2016. A clinical approach to diagnosis of autoimmune encephalitis. Lancet Neurol. 15, 391–404. https://doi.org/10.1016/S1474-4422(15)00401-9.

Hanly, J.G., Urowitz, M.B., Su, L., Bae, S.C., Gordon, C., Clarke, A., Bernatsky, S., Vasudevan, A., Isenberg, D., Rahman, A., Wallace, D.J., Fortin, P.R., Gladman, D., Romero-Diaz, J., Sanchez-Guerrero, J., Dooley, M.A., Bruce, I., Steinsson, K., Khamashta, M., Manzi, S., Ramsey-Goldman, R., Sturfelt, G., Nived, O., van Vollenhoven, R., Ramos-Casals, M., Aranow, C., Mackay, M., Kalunian, K., Alarcon, G.S., Fessler, B.J., Ruiz-Irastorza, G., Petri, M., Lim, S., Kamen, D., Peschken, C., Farewell, V., Thompson, K., Theriault, C., Merrill, J.T., 2011. Autoantibodies as biomarkers for the prediction of neuropsychiatric events in systemic lupus erythematosus. Ann. Rheum. Dis. 70, 1726–1732. https://doi.org/10.1136/ard.2010.148502.

Hansen, H.C., Klingbeil, C., Dalmau, J., Li, W., Weissbrich, B., Wandinger, K.P., 2013. Persistent intrathecal antibody synthesis 15 years after recovering from anti-N-methyl-D-aspartate receptor encephalitis. JAMA Neurol. 70, 117–119. https://doi.org/10.1001/jamaneurol.2013.585.

Harding, K., Williams, O., Willis, M., Hrastelj, J., Rimmer, A., Joseph, F., Tomassini, V., Wardle, M., Pickersgill, T., Robertson, N., Tallantyre, E., 2019. Clinical outcomes of escalation vs early intensive disease-modifying therapy in patients with multiple sclerosis. JAMA Neurol. 76, 536–541. https://doi.org/10.1001/jamaneurol.2018.4905.

He, A., Merkel, B., Brown, J.W.L., Zhovits Ryerson, L., Kister, I., Malpas, C.B., Sharmin, S., Horakova, D., Kubala Havrdova, E., Spelman, T., Izquierdo, G., Eichau, S., Trojano, M., Lugaresi, A., Hupperts, R., Sola, P., Ferraro, D., Lycke, J., Grand'Maison, F., Prat, A., Girard, M., Duquette, P., Larochelle, C., Svenningsson, A., Petersen, T., Grammond, P., Granella, F., Van Pesch, V., Bergamaschi, R., McGuigan, C., Coles, A., Hillert, J., Piehl, F., Butzkueven, H., Kalincik, T., 2020. Timing of high-efficacy therapy for multiple sclerosis: a retrospective observational cohort study. Lancet Neurol. 19, 307–316. https://doi.org/10.1016/S1474-4422(20)30067-3.

Hjalmarsson, A., Blomqvist, P., Skoldenberg, B., 2007. Herpes simplex encephalitis in Sweden, 1990-2001: incidence, morbidity, and mortality. Clin. Infect. Dis. 45, 875–880. https://doi.org/10.1086/521262.

Hughes, E.G., Peng, X., Gleichman, A.J., Lai, M., Zhou, L., Tsou, R., Parsons, T.D., Lynch, D.R., Dalmau, J., Balice-Gordon, R.J., 2010. Cellular and synaptic mechanisms of anti-NMDA receptor encephalitis. J. Neurosci. 30, 5866–5875. https://doi.org/10.1523/JNEUROSCI.0167-10.2010.

Hummert, M.W., Jendretzky, K.F., Fricke, K., Gingele, M., Ratuszny, D., Mohn, N., Trebst, C., Skripuletz, T., Gingele, S., Suhs, K.W., 2023. The relevance of NMDA receptor antibody-specific index for diagnosis and prognosis in patients with anti-NMDA receptor encephalitis. Sci. Rep. 13, 12696. https://doi.org/10.1038/s41598-023-38462-6.

Hunter, D., Petit-Pedrol, M., Fernandes, D., Benac, N., Rodrigues, C., Kreye, J., Ceanga, M., Pruss, H., Geis, C., Groc, L., 2024. Converging synaptic and network dysfunctions in distinct autoimmune encephalitis. EMBO Rep. 25, 1623–1649. https://doi.org/10.1038/s44319-024-00056-2.

James, C., Harfouche, M., Welton, N.J., Turner, K.M., Abu-Raddad, L.J., Gottlieb, S.L., Looker, K.J., 2020. Herpes simplex virus: global infection prevalence and incidence estimates, 2016. Bull. World Health Organ. 98, 315–329. https://doi.org/10.2471/BLT.19.237149.

Jeong, J.S., Jiang, L., Albino, E., Marrero, J., Rho, H.S., Hu, J., Hu, S., Vera, C., Bayron-Poueymiroy, D., Rivera-Pacheco, Z.A., Ramos, L., Torres-Castro, C., Qian, J., Bonaventura, J., Boeke, J.D., Yap, W.Y., Pino, I., Eichinger, D.J., Zhu, H., Blackshaw, S., 2012. Rapid identification of monospecific monoclonal antibodies using a human proteome microarray. Mol. Cell. Proteomics 11 (O111), 016253. https://doi.org/10.1074/mcp.O111.016253.

Johnson, T.P., Larman, H.B., Lee, M.H., Whitehead, S.S., Kowalak, J., Toro, C., Lau, C.C., Kim, J., Johnson, K.R., Reoma, L.B., Faustin, A., Pardo, C.A., Kottapalli, S., Howard, J., Monaco, D., Weisfeld-Adams, J., Blackstone, C., Galetta, S., Snuderl, M., Gahl, W.A., Kister, I., Nath, A., 2019. Chronic dengue virus panencephalitis in a patient with progressive dementia with extrapyramidal features. Ann. Neurol. 86, 695–703. https://doi.org/10.1002/ana.25588.

Jouan, Y., Grammatico-Guillon, L., Espitalier, F., Cazals, X., Francois, P., Guillon, A., 2015. Long-term outcome of severe herpes simplex encephalitis: a population-based observational study. Crit. Care 19, 345. https://doi.org/10.1186/s13054-015-1046-y.

Kreye, J., Wenke, N.K., Chayka, M., Leubner, J., Murugan, R., Maier, N., Jurek, B., Ly, L. T., Brandl, D., Rost, B.R., Stumpf, A., Schulz, P., Radbruch, H., Hauser, A.E., Pache, F., Meisel, A., Harms, L., Paul, F., Dirnagl, U., Garner, C., Schmitz, D., Wardemann, H., Pruss, H., 2016. Human cerebrospinal fluid monoclonal N-methyl-D-aspartate receptor autoantibodies are sufficient for encephalitis pathogenesis. Brain 139, 2641–2652. https://doi.org/10.1093/brain/aww208.

Kreye, J., Wright, S.K., van Casteren, A., Stoffler, L., Machule, M.L., Reincke, S.M., Nikolaus, M., van Hoof, S., Sanchez-Sendin, E., Homeyer, M.A., Cordero Gomez, C., Kornau, H.C., Schmitz, D., Kaindl, A.M., Boehm-Sturm, P., Mueller, S., Wilson, M.A., Upadhya, M.A., Dhangar, D.R., Greenhill, S., Woodhall, G., Turko, P., Vida, I., Garner, C.C., Wickel, J., Geis, C., Fukata, Y., Fukata, M., Pruss, H., 2021. Encephalitis patient-derived monoclonal GABAA receptor antibodies cause epileptic seizures. J. Exp. Med. 218. https://doi.org/10.1084/jem.20210012.

Larman, H.B., Laserson, U., Querol, L., Verhaeghen, K., Solimini, N.L., Xu, G.J., Klarenbeek, P.L., Church, G.M., Hafler, D.A., Plenge, R.M., Nigrovic, P.A., De Jager, P.L., Weets, I., Martens, G.A., O'Connor, K.C., Elledge, S.J., 2013. PhIP-Seq characterization of autoantibodies from patients with multiple sclerosis, type 1 diabetes and rheumatoid arthritis. J. Autoimmun. 43, 1–9. https://doi.org/10.1016/j.jaut.2013.01.013.

Larman, H.B., Zhao, Z., Laserson, U., Li, M.Z., Ciccia, A., Gakidis, M.A., Church, G.M., Kesari, S., Leproust, E.M., Solimini, N.L., Elledge, S.J., 2011. Autoantigen discovery with a synthetic human peptidome. Nat. Biotechnol. 29, 535–541. https://doi.org/10.1038/nbt.1856.

Le Bon, A., Schiavoni, G., D'Agostino, G., Gresser, I., Belardelli, F., Tough, D.F., 2001. Type i interferons potently enhance humoral immunity and can promote isotype switching by stimulating dendritic cells in vivo. Immunity 14, 461–470. https://doi.org/10.1016/s1074-7613(01)00126-1.

Leib, D.A., 2002. Counteraction of interferon-induced antiviral responses by herpes simplex viruses. Curr. Top. Microbiol. Immunol. 269, 171–185. https://doi.org/10.1007/978-3-642-59421-2_11.

Leypoldt, F., Hoftberger, R., Titulaer, M.J., Armangue, T., Gresa-Arribas, N., Jahn, H., Rostasy, K., Schlumberger, W., Meyer, T., Wandinger, K.P., Rosenfeld, M.R., Graus, F., Dalmau, J., 2015. Investigations on CXCL13 in anti-N-methyl-D-aspartate receptor encephalitis: a potential biomarker of treatment response. JAMA Neurol. 72, 180–186. https://doi.org/10.1001/jamaneurol.2014.2956.

Liebhoff, A.M., Venkataraman, T., Morgenlander, W.R., Na, M., Kula, T., Waugh, K., Morrison, C., Rewers, M., Longman, R., Round, J., Elledge, S., Ruczinski, I., Langmead, B., Larman, H.B., 2024. Efficient encoding of large antigenic spaces by epitope prioritization with Dolphyn. Nat. Commun. 15, 1577. https://doi.org/10.1038/s41467-024-45601-8.

Mesev, E.V., LeDesma, R.A., Ploss, A., 2019. Decoding type I and III interferon signalling during viral infection. Nat. Microbiol. 4, 914–924. https://doi.org/10.1038/s41564-019-0421-x.

Mohan, D., Wansley, D.L., Sie, B.M., Noon, M.S., Baer, A.N., Laserson, U., Larman, H.B., 2018. PhIP-Seq characterization of serum antibodies using oligonucleotide-encoded peptidomes. Nat. Protoc. 13, 1958–1978. https://doi.org/10.1038/s41596-018-0025-6.

Monaco, D.R., Sie, B.M., Nirschl, T.R., Knight, A.C., Sampson, H.A., Nowak-Wegrzyn, A., Wood, R.A., Hamilton, R.G., Frischmeyer-Guerrerio, P.A., Larman, H.B., 2021. Profiling serum antibodies with a pan allergen phage library identifies key wheat allergy epitopes. Nat. Commun. 12, 379. https://doi.org/10.1038/s41467-020-20622-1.

Morgenlander, W.R., 2022. ARscore. GitHub.

Morgenlander, W.R., Chia, W.N., Parra, B., Monaco, D.R., Ragan, I., Pardo, C.A., Bowen, R., Zhong, D., Norris, D.E., Ruczinski, I., Durbin, A., Wang, L.F., Larman, H. B., Robinson, M.L., 2024. Precision arbovirus serology with a pan-arbovirus peptidome. Nat. Commun. 15, 5833. https://doi.org/10.1038/s41467-024-49461-0.

Nosadini, M., Eyre, M., Molteni, E., Thomas, T., Irani, S.R., Dalmau, J., Dale, R.C., Lim, M., Anlar, B., Armangue, T., Benseler, S., Cellucci, T., Deiva, K., Gallentine, W., Gombolay, G., Gorman, M.P., Hacohen, Y., Jiang, Y., Lim, B.C., Muscal, E., Ndondo, A., Neuteboom, R., Rostasy, K., Sakuma, H., Sartori, S., Sharma, S., Tenembaum, S.N., Van Mater, H.A., Wells, E., Wickstrom, R., Yeshokumar, A.K., 2021. Use and safety of immunotherapeutic management of N-Methyl-d-aspartate receptor antibody encephalitis: a meta-analysis. JAMA Neurol. 78, 1333–1344. https://doi.org/10.1001/jamaneurol.2021.3188.

Nosadini, M., Mohammad, S.S., Corazza, F., Ruga, E.M., Kothur, K., Perilongo, G., Frigo, A.C., Toldo, I., Dale, R.C., Sartori, S., 2017. Herpes simplex virus-induced anti-N-methyl-d-aspartate receptor encephalitis: a systematic literature review with analysis of 43 cases. Dev. Med. Child Neurol. 59, 796–805. https://doi.org/10.1111/dmcn.13448.

Pfeffer, L.M., 2011. The role of nuclear factor kappaB in the interferon response. J. Interferon Cytokine Res. 31, 553–559. https://doi.org/10.1089/jir.2011.0028.

Pinal-Fernandez, I., Casal-Dominguez, M., Derfoul, A., Pak, K., Miller, F.W., Milisenda, J. C., Grau-Junyent, J.M., Selva-O'Callaghan, A., Carrion-Ribas, C., Paik, J.J., Albayda, J., Christopher-Stine, L., Lloyd, T.E., Corse, A.M., Mammen, A.L., 2020. Machine learning algorithms reveal unique gene expression profiles in muscle biopsies from patients with different types of myositis. Ann. Rheum. Dis. 79, 1234–1242. https://doi.org/10.1136/annrheumdis-2019-216599.

Pinal-Fernandez, I., Munoz-Braceras, S., Casal-Dominguez, M., Pak, K., Torres-Ruiz, J., Musai, J., Dell'Orso, S., Naz, F., Islam, S., Gutierrez-Cruz, G., Cano, M.D., Matas-

Garcia, A., Padrosa, J., Tobias-Baraja, E., Garrabou, G., Aldecoa, I., Espinosa, G., Simeon-Aznar, C.P., Guillen-Del-Castillo, A., Gil-Vila, A., Trallero-Araguas, E., Christopher-Stine, L., Lloyd, T.E., Liewluck, T., Naddaf, E., Stenzel, W., Greenberg, S. A., Grau, J.M., Selva-O'Callaghan, A., Milisenda, J.C., Mammen, A.L., 2024. Pathological autoantibody internalisation in myositis. Ann. Rheum. Dis. 83, 1549–1560. https://doi.org/10.1136/ard-2024-225773.

Planaguma, J., Leypoldt, F., Mannara, F., Gutierrez-Cuesta, J., Martin-Garcia, E., Aguilar, E., Titulaer, M.J., Petit-Pedrol, M., Jain, A., Balice-Gordon, R., Lakadamyali, M., Graus, F., Maldonado, R., Dalmau, J., 2015. Human N-methyl D-aspartate receptor antibodies alter memory and behaviour in mice. Brain 138, 94–109. https://doi.org/10.1093/brain/awu310.

Pruss, H., 2021. Autoantibodies in neurological disease. Nat. Rev. Immunol. 21, 798–813. https://doi.org/10.1038/s41577-021-00543-w.

Pruss, H., Finke, C., Holtje, M., Hofmann, J., Klingbeil, C., Probst, C., Borowski, K., Ahnert-Hilger, G., Harms, L., Schwab, J.M., Ploner, C.J., Komorowski, L., Stoecker, W., Dalmau, J., Wandinger, K.P., 2012. N-methyl-D-aspartate receptor antibodies in herpes simplex encephalitis. Ann. Neurol. 72, 902–911. https://doi.org/10.1002/ana.23689.

Reiber, H., 1998. Cerebrospinal fluid–physiology, analysis and interpretation of protein patterns for diagnosis of neurological diseases. Mult. Scler. 4, 99–107. https://doi.org/10.1177/135245859800400302.

Reiber, H., Felgenhauer, K., 1987. Protein transfer at the blood cerebrospinal fluid barrier and the quantitation of the humoral immune response within the central nervous system. Clin. Chim. Acta 163, 319–328. https://doi.org/10.1016/0009-8981(87)90250-6.

Reiber, H., Lange, P., 1991. Quantification of virus-specific antibodies in cerebrospinal fluid and serum: sensitive and specific detection of antibody synthesis in brain. Clin. Chem. 37, 1153–1160.

Rocchi, A., Sacchetti, S., De Fusco, A., Giovedi, S., Parisi, B., Cesca, F., Holtje, M., Ruprecht, K., Ahnert-Hilger, G., Benfenati, F., 2019. Autoantibodies to synapsin I sequestrate synapsin I and alter synaptic function. Cell Death Dis. 10, 864. https://doi.org/10.1038/s41419-019-2106-z.

Rodriguez-Mogeda, C., van Gool, M.M., van der Mast, R., Nijland, R., Keasberry, Z., van de Bovekamp, L., van Delft, M.A., Picon, C., Reynolds, R., Killestein, J., Teunissen, C. E., de Vries, H.E., van Egmond, M., Witte, M.E., 2024. Intrathecal IgG and IgM synthesis correlates with neurodegeneration markers and corresponds to meningeal B cell presence in MS. Sci. Rep. 14, 25540. https://doi.org/10.1038/s41598-024-76969-8.

Salovin, A., Glanzman, J., Roslin, K., Armangue, T., Lynch, D.R., Panzer, J.A., 2018. Anti-NMDA receptor encephalitis and nonencephalitic HSV-1 infection. Neurol. Neuroimmunol. Neuroinflamm. 5, e458.

Shamier, M.C., Bogers, S., Yusuf, E., van Splunter, M., Ten Berge, J., Titulaer, M., van Kampen, J.J.A., GeurtsvanKessel, C.H., 2021. The role of antibody indexes in clinical virology. Clin. Microbiol. Infect. 27, 1207–1211. https://doi.org/10.1016/j.cmi.2021.03.015.

Sili, U., Kaya, A., Mert, A., 2014. Herpes simplex virus encephalitis: clinical manifestations, diagnosis and outcome in 106 adult patients. J. Clin. Virol. 60, 112–118. https://doi.org/10.1016/j.jcv.2014.03.010.

Singh, T.D., Fugate, J.E., Hocker, S., Wijdicks, E.F.M., Aksamit Jr., A.J., Rabinstein, A.A., 2016. Predictors of outcome in HSV encephalitis. J. Neurol. 263, 277–289. https://doi.org/10.1007/s00415-015-7960-8.

Sjoberg, R., Mattsson, C., Andersson, E., Hellstrom, C., Uhlen, M., Schwenk, J.M., Ayoglu, B., Nilsson, P., 2016. Exploration of high-density protein microarrays for antibody validation and autoimmunity profiling. N. Biotechnol. 33, 582–592. https://doi.org/10.1016/j.nbt.2015.09.002.

Stahl, J.P., Mailles, A., De Broucker, T., Steering, C., Investigators, G., 2012. Herpes simplex encephalitis and management of acyclovir in encephalitis patients in France. Epidemiol. Infect. 140, 372–381. https://doi.org/10.1017/S0950268811000483.

Steiner, I., 2011. Herpes simplex virus encephalitis: new infection or reactivation? Curr. Opin. Neurol. 24, 268–274. https://doi.org/10.1097/WCO.0b013e328346be6f.

Thompson, A.J., Banwell, B.L., Barkhof, F., Carroll, W.M., Coetzee, T., Comi, G., Correale, J., Fazekas, F., Filippi, M., Freedman, M.S., Fujihara, K., Galetta, S.L., Hartung, H.P., Kappos, L., Lublin, F.D., Marrie, R.A., Miller, A.E., Miller, D.H., Montalban, X., Mowry, E.M., Sorensen, P.S., Tintore, M., Traboulsee, A.L., Trojano, M., Uitdehaag, B.M.J., Vukusic, S., Waubant, E., Weinshenker, B.G., Reingold, S.C., Cohen, J.A., 2018. Diagnosis of multiple sclerosis: 2017 revisions of the McDonald criteria. Lancet Neurol. 17, 162–173. https://doi.org/10.1016/S1474-4422(17)30470-2.

Titulaer, M.J., McCracken, L., Gabilondo, I., Armangue, T., Glaser, C., Iizuka, T., Honig, L.S., Benseler, S.M., Kawachi, I., Martinez-Hernandez, E., Aguilar, E., Gresa-Arribas, N., Ryan-Florance, N., Torrents, A., Saiz, A., Rosenfeld, M.R., Balice-Gordon, R., Graus, F., Dalmau, J., 2013. Treatment and prognostic factors for long-term outcome in patients with anti-NMDA receptor encephalitis: an observational cohort study. Lancet Neurol. 12, 157–165. https://doi.org/10.1016/S1474-4422(12)70310-1.

Tucker, D.F., Sullivan, J.T., Mattia, K.A., Fisher, C.R., Barnes, T., Mabila, M.N., Wilf, R., Sulli, C., Pitts, M., Payne, R.J., Hall, M., Huston-Paterson, D., Deng, X., Davidson, E., Willis, S.H., Doranz, B.J., Chambers, R., Rucker, J.B., 2018. Isolation of state-dependent monoclonal antibodies against the 12-transmembrane domain glucose transporter 4 using virus-like particles. PNAS 115, E4990–E4999. https://doi.org/10.1073/pnas.1716788115.

Venkatesan, A., Michael, B.D., Probasco, J.C., Geocadin, R.G., Solomon, T., 2019. Acute encephalitis in immunocompetent adults. Lancet 393, 702–716. https://doi.org/10.1016/S0140-6736(18)32526-1.

Vogl, T., Klompus, S., Leviatan, S., Kalka, I.N., Weinberger, A., Wijmenga, C., Fu, J., Zhernakova, A., Weersma, R.K., Segal, E., 2021. Population-wide diversity and stability of serum antibody epitope repertoires against human microbiota. Nat. Med. 27, 1442–1450. https://doi.org/10.1038/s41591-021-01409-3.

Wang, E.Y., Dai, Y., Rosen, C.E., Schmitt, M.M., Dong, M.X., Ferre, E.M.N., Liu, F., Yang, Y., Gonzalez-Hernandez, J.A., Meffre, E., Hinchcliff, M., Koumpouras, F., Lionakis, M.S., Ring, A.M., 2022. High-throughput identification of autoantibodies that target the human exoproteome. Cell Rep. Methods 2. https://doi.org/10.1016/j.crmeth.2022.100172.

Warnke, C., von Geldern, G., Markwerth, P., Dehmel, T., Hoepner, R., Gold, R., Pawlita, M., Kumpfel, T., Maurer, M., Stangel, M., Wegner, F., Hohlfeld, R., Straeten, V., Limmroth, V., Weber, T., Hermsen, D., Kleinschnitz, C., Hartung, H.P., Wattjes, M.P., Svenningson, A., Major, E., Olsson, T., Kieseier, B.C., Adams, O., 2014. Cerebrospinal fluid JC virus antibody index for diagnosis of natalizumab-associated progressive multifocal leukoencephalopathy. Ann. Neurol. 76, 792–801. https://doi.org/10.1002/ana.24153.

Whitfield, T., Fernandez, C., Davies, K., Defres, S., Griffiths, M., Hooper, C., Tangney, R., Burnside, G., Rosala-Hallas, A., Moore, P., Das, K., Zuckerman, M., Parkes, L., Keller, S., Roberts, N., Easton, A., Touati, S., Kneen, R., Stahl, J.P., Solomon, T., 2021. Protocol for DexEnceph: a randomised controlled trial of dexamethasone therapy in adults with herpes simplex virus encephalitis. BMJ Open 11, e041808. https://doi.org/10.1136/bmjopen-2020-041808.

Wright, S.K., Rosch, R.E., Wilson, M.A., Upadhya, M.A., Dhangar, D.R., Clarke-Bland, C., Wahid, T.T., Barman, S., Goebels, N., Kreye, J., Pruss, H., Jacobson, L., Bassett, D.S., Vincent, A., Greenhill, S.D., Woodhall, G.L., 2021. Multimodal electrophysiological analyses reveal that reduced synaptic excitatory neurotransmission underlies seizures in a model of NMDAR antibody-mediated encephalitis. Commun. Biol. 4, 1106. https://doi.org/10.1038/s42003-021-02635-8.

Xing, J., Ni, L., Wang, S., Wang, K., Lin, R., Zheng, C., 2013. Herpes simplex virus 1-encoded tegument protein VP16 abrogates the production of beta interferon (IFN) by inhibiting NF-kappaB activation and blocking IFN regulatory factor 3 to recruit its coactivator CBP. J. Virol. 87, 9788–9801. https://doi.org/10.1128/JVI.01440-13.

Xu, G.J., Kula, T., Xu, Q., Li, M.Z., Vernon, S.D., Ndung'u, T., Ruxrungtham, K., Sanchez, J., Brander, C., Chung, R.T., O'Connor, K.C., Walker, B., Larman, H.B., Elledge, S.J., 2015. Viral immunology. Comprehensive serological profiling of human populations using a synthetic human virome. Science 348, aaa0698. https://doi.org/10.1126/science.aaa0698.

Xu, G.J., Shah, A.A., Li, M.Z., Xu, Q., Rosen, A., Casciola-Rosen, L., Elledge, S.J., 2016. Systematic autoantigen analysis identifies a distinct subtype of scleroderma with coincident cancer. PNAS 113, E7526–E7534. https://doi.org/10.1073/pnas.1615990113.

Zhang, J., Wang, S., Wang, K., Zheng, C., 2013. Herpes simplex virus 1 DNA polymerase processivity factor UL42 inhibits TNF-alpha-induced NF-kappaB activation by interacting with p65/RelA and p50/NF-kappaB1. Med. Microbiol. Immunol. 202, 313–325. https://doi.org/10.1007/s00430-013-0295-0.

Zheng, Z., Sohn, S., Ahn, K.J., Bang, D., Cho, S.B., 2015. Serum reactivity against herpes simplex virus type 1 UL48 protein in Behcet's disease patients and a Behcet's disease-like mouse model. Acta Derm. Venereol. 95, 952–958. https://doi.org/10.2340/00015555-2127.

Jayaraman, S, Tiniakou, E., Morgenlander, W.R., Na, M., Christopher-Stine, L., Larman, H.B., 2025. Comprehensive Enteroviral Serology Links Infection and Anti-Melanoma Differentiation-Associated Protein 5 Dermatomyositis. ACR Open Rheumatol. 2025 Jan;7(1):e11752. doi: 10.1002/acr2.11752.